Psychological Review
2002, Vol. 109, No. 3, 545–572

0033-295X/02/$5.00 DOI: 10.1037//0033-295X.109.3.545

Dynamic Field Theory of Movement Preparation

Wolfram Erlhagen
Ruhr-Universität Bochum

Gregor Schöner
C.N.R.S. Marseille

A theoretical framework for understanding movement preparation is proposed. Movement parameters are represented by activation fields, distributions of activation defined over metric spaces. The fields evolve under the influence of various sources of localized input, representing information about upcoming movements. Localized patterns of activation self-stabilize through cooperative and competitive interactions within the fields. The task environment is represented by a 2nd class of fields, which preshape the movement parameter representation. The model accounts for a sizable body of empirical findings on movement initiation (continuous and graded nature of movement preparation, dependence on the metrics of the task, stimulus uncertainty effect, stimulus–response compatibility effects, Simon effect, precuing paradigm, and others) and suggests new ways of exploring the structure of motor representations.

Consider a person reaching for an object in his or her vicinity. In the conventional analysis, this act involves a number of processes that can be described by roughly following the flow of sensory information: (a) The person senses light reflected from the surface of the object; (b) from this sensory stimulation, the individual extracts invariants that uniquely characterize the object; (c) he or she assembles the set of parameter values that specify the required reaching and grasping movements; (d) the individual meters these parameters out in time and sets up his or her neuromuscular system to control the movement; and (e) the skeletomuscular system executes the movement. Traditionally, researchers have dealt with these partially overlapping processes within two separate categories. They analyzed processes taking place before movement initiation in terms of concepts of information processing and representation but addressed the processes of control and execution of movement based on control theory and biomechanics. This difference in the theoretical frameworks was associated with different experimental methods. Researchers typically assessed movement preparation, including the relevant sensory and perceptual processes, through measurement of reaction times, analysis of error, and systematic manipulation of the information content of stimulation and task setting. By contrast, they studied control and execution by measuring movement trajectories, by looking at their dependence on conditions of feedback, of load, of place in articulatory space, and so on. (For general reviews of the organization of voluntary movement, see Georgopoulos, 1986, 1991; Ghez, Hening, & Gordon, 1991; Keele, 1981, 1986; Poulton, 1981; Rosenbaum, 1991.)

Over the past few years both theoretical and experimental developments have continued to call this traditional view into question. Modelers have used the concept of computation across both domains (e.g., to address control problems as in Jordan, 1990, or to address how movements are assembled and represented as in Rosenbaum, Loukopoulos, Meulenbroek, Vaughan, & Engelbrecht, 1995). More generally, connectionist modelers have demonstrated that movement planning can be described based on distributed, nonsymbolic representations (e.g., Hinton, 1984) on which temporally graded subsymbolic computation takes place. In the domain of motor control, modelers have used concepts from nonlinear dynamical systems to describe not only how movements are coordinated but also how switches between different patterns of coordination are brought about (Schöner & Kelso, 1988a, 1988b). They have thus shown that coordinating movement is a problem not only of motor control but also of movement planning, that is, of selecting particular movement patterns.

Most important, experimental lines of evidence too suggest that the two domains are much more intimately linked than previously thought. For instance, on-line updating of planned movements (e.g., Goodale, Pélisson, & Prablanc, 1986; Prablanc & Martin,

Wolfram Erlhagen, Institut für Neuroinformatik, Ruhr-Universität Bochum, Bochum, Germany; Gregor Schöner, Centre de Recherche en Neurosciences Cognitives, C.N.R.S. Marseille, Marseille, France.

Wolfram Erlhagen is now at the Department of Mathematics, University of Minho, Braga, Portugal.

Support from Deutsche Forschungsgemeinschaft, Germany, Grants Scho 336/3-1, Scho 336/4-2, and Er 246/1-3 and the Groupement d'Intérêt Scientifique Science de la Cognition, France, is gratefully acknowledged. Part of this work was performed during multiple visits of Gregor Schöner to the Department of Psychology at Indiana University with partial support from the Cognitive Science program and from Esther Thelen. The institutional support provided by Werner von Seelen at the Institut für Neuroinformatik, Bochum, Germany, is gratefully acknowledged.

We thank Klaus Kopecz and Christoph Engels for their contributions to our understanding of neural field ideas, and Martin Giese, Axel Steinhage, Alexa Riehle, Annette Bastian, and John Jeka for discussions. Special thanks and fond remembrance go to the late Jean Requin, who intensively discussed some of these ideas with Gregor Schöner. Discussions and encouragement from Esther Thelen and Linda Smith pushed us along. Esther Thelen thoroughly read different versions of this article. We thank Claude Ghez for making then unpublished results available and David Rosenbaum for helpful comments on an earlier version of this article.

Correspondence concerning this article should be addressed to Gregor Schöner, who is now at the Institut für Neuroinformatik, Ruhr-Universität Bochum, Lehrstuhl für Theoretische Biologie, Gebäude ND 04/584, 44780 Bochum, Germany. E-mail: gregor.schoener@neuroinformatik.ruhr-uni-bochum.de

1992) may occur at any time during the movement preparation or execution processes. The gradual and continuous nature of movement preparation has been made directly visible by Claude Ghez and his colleagues (for reviews, see Favilla, Gordon, Ghilardi, & Ghez, 1990; Favilla, Gordon, Hening, & Ghez, 1990; Favilla, Hening, & Ghez, 1989; Ghez, Hening, & Favilla, 1990; Hening, Favilla, & Ghez, 1988) using the timed movement initiation paradigm (Schouten & Bekker, 1967). These results are central to the arguments we present in this article. They show that the process of specification of voluntary movements evolves continuously in time and depends on the task environment.

We believe that the conceptual divide between the domain of movement preparation and motor control is no longer tenable. The goal of this article is, therefore, to provide a new theoretical framework in which movement preparation can be understood in terms compatible with the control theoretical concepts used to describe movement execution. The theoretical concepts are based on the theory of nonlinear dynamical systems, emphasizing attractor states and their bifurcations, but are appropriately generalized to spatially extended systems so as to do justice to the particular characteristics of representational systems. We refer to this set of theoretical concepts as the *dynamic field theory of movement preparation.* The three main ideas are as follows. First, movements are represented by continuous, subsymbolic distributions of activation defined over the space of movement parameters. Second, movement preparation is the continuous evolution in time of these distributions as described by a nonlinear dynamical system. This dynamical system integrates different sources of specification and generates a decision about the upcoming movement on the basis of strong interaction within the activation distributions. Third, the task environment is represented by a second, similar distribution of activation, which is structured by various sources of information about possible movements. One such source is a memory trace of activation distributions, representing the recent motor history.

Because control theory and attractor dynamics are constructed around the shared concept of stability, this framework bridges the conceptual divide between movement preparation and motor control. By conceiving of the movement plan as a stable stationary state based on current sensory information, the continuous on-line updating of planned movements can be accounted for. The new account improves classical theoretical thinking about the processes underlying behavioral choice (reviewed by Grice, Nullmeyer, & Spiker, 1982; Luce, 1986) by addressing the question of how the different behavioral choices are set up, that is, how the task environment becomes part of the information-processing system. On this basis, we derive many classical results in the reaction time literature, such as the increase of reaction time with increasing number of stimulus–response pairings (stimulus uncertainty effect) as well as stimulus–response compatibility effects. We delineate the range of validity of these classical effects, predicting their breakdown under specific conditions.

More important, by providing an account for how movement parameters are specified continuously in time and gradually in parameter value, as observed by Ghez and colleagues (Ghez et al., 1990), we are led to new questions. We show, for instance, how the dependence of reaction time on the metrics of the movement task arises naturally in our account, although this dependence cannot be understood on the basis of abstract information processes. Similarly, we demonstrate how probabilities of choice alone fail in predicting reaction time. We give a new interpretation to the results from the Rosenbaum (1980) paradigm, tracing inherent differences between movement parameters such as direction or amplitude to differences in the metrics of the movement task.

We proceed as follows: The next section presents the basic concepts of the theoretical language of dynamic neural fields and spells out a model of movement preparation in those terms. Predictions of the theory are then first derived while taking only a single movement parameter into account. Multidimensional representations are considered next. We close the article with a critical discussion of a number of conceptual implications of our model. Some technical details are treated in four appendixes.

The Basic Concepts of Dynamic Field Theory

Movement Parameters and the Movement Parameter Space

A movement act as a whole can be characterized by a number of parameters, such as the extent (or amplitude) of the movement, the spatial direction of the movement, its peak velocity, the maximal level of force needed to overcome resistance, the curvature of the trajectory, the amount of involvement of different effectors, and so on. Some of these parameters (e.g., direction) are well-defined from the start of the movement, so that the specification of the values of those parameters must occur before movement initiation. Quite generally, and independent of exactly how the movement is realized and controlled, the specification of any particular movement act can be viewed as the process of assigning particular values to these parameters. All of these parameters are continuous and have a natural metric based on the physical description of the movement act. This continuous and metric description is relevant for the description of the process of specification of a movement act, because people can generate a corresponding continuum of different movement acts.

Each movement parameter defines an abstract dimension, which one can think of as an axis in a potentially high-dimensional parameter space. Any particular movement act corresponds to a point in that space. For each individual movement parameter we may thus specify a particular value along the corresponding axis of the parameter space. Consider, for example, straight-line movement of the hand in a plane. The direction of that movement is a movement parameter, which defines one axis in the space of movement parameters. Each such movement in any given direction corresponds to a particular value of the parameter of direction, or, equivalently, to a particular location along an axis spanned by that parameter. If in different trials different movement directions are realized, each different movement corresponds to a different location along that axis.

The Activation Field

To fix ideas, we consider for the moment only one movement parameter, x, say direction in the context of planar movement. (Later, in the Multidimensional Dynamic Fields: Specifying Multiple Parameters section, we move beyond this simplification.) To represent a particular value of the movement parameter, say, movement at 90° from some reference direction, we introduce an activation variable, $u(90)$. High levels of activation indicate that

the particular value is specified; low levels of activation indicate that the particular value is not currently involved in the specification of the movement. There is one activation variable, $u(x)$, for each possible value of the movement parameter, x. Because the parameter spans a continuous space, this means that there are continuously many variables, one for each point on the parameter axis. This is called an *activation field.* (This mathematical concept is familiar from physics, where, for instance, the electrical potential is a field associating a value, the potential, with every point in three-dimensional space.)

Different states of affairs can be expressed with this field notion (see Figure 1). A localized distribution of activation (see Figure 1a) represents a particular unique value of the movement parameter. A flat, homogeneous state of the field (see Figure 1b) represents the absence of information about any particular value of the movement parameter. Graded information about the movement parameter is represented by other, appropriately shaped distributions of activation. For example, the pattern of activation illustrated in Figure 1c represents a state of affairs in which two ranges of values of the parameter of direction are currently specified. The left-most range is less strongly activated than the right-most range.

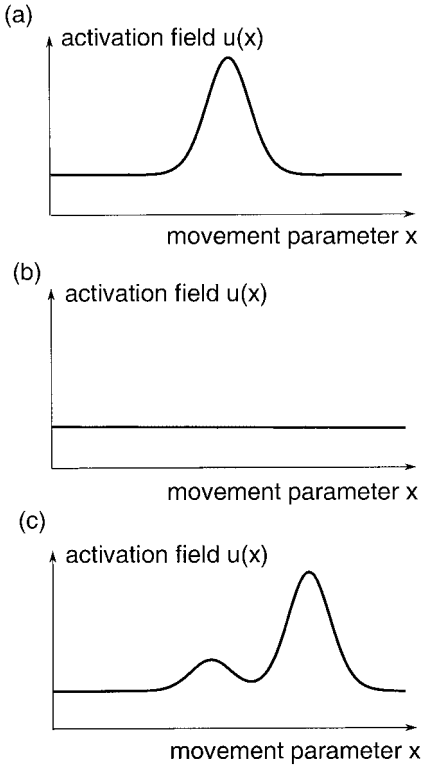

Figure 1. Different states of affairs can be expressed by the activation field. (a) A unique value of the movement parameter is represented by the location of a single peak of activation. (b) The absence of any information about the underlying dimension of the motor act is expressed by a homogeneous distribution of activation. (c) More complex patterns of activation represent graded information about multiple values of the movement parameter.

Field Dynamics

Specifying a motor act corresponds to specifying a particular pattern of activation for the field representing the movement parameter. We assume that changes of activation in the field occur continuously in time. Under some mild additional assumptions this means that the activation field is the solution of a dynamical system (e.g., Arnold, 1973), so that the rate of change of the activation field, $\dot{u}(x, t) = du(x, t)/dt$, where t is time, is a function of the current state of the field:

$$\dot{u}(x, t) = f[u(x', t)], \tag{1}$$

where the brackets indicate that the function may depend on the activation at any site, x', of the field, not just on the activation at the site, x, at which we determine the rate of change. This very formal way of defining things is not particularly useful. To be more specific, we first consider the case in which the field evolves independently at each site. A simple description is

$$\tau\dot{u}(x, t) = -u(x, t) + h + S(x, t), \tag{2}$$

in which the parameter τ fixes the time scale of the evolution of activation. In the absence of input, $S(x, t) = 0$, this linear dynamical system (illustrated in Figure 2, black line) has a stable (attractor) solution at the resting level, h: $u(x, t) = h < 0$. The system converges in time to this resting level from any initial level of activation.[1] When input, $S(x) > 0$, is added (see gray line in Figure 2), the attractor state shifts to the larger level of activation, $u(x) = S(x) + h$. The relaxation process automatically drives activation to that level. Even an abrupt change of input thus leads to a continuous change of activation.

Many models of information or neural processing postulate that when activation is increased beyond some boundary or threshold level, information is transmitted. In our approach, the "off" and "on" levels of activation are inherent, qualitatively different states of the activation dynamics. This is achieved by making the dynamical system strongly nonlinear:

$$\tau\dot{u}(x, t) = -u(x, t) + h + S(x, t) + f[u(x, t)], \tag{3}$$

where $f(u)$ is a sigmoidal nonlinearity defined below. This dynamical system is illustrated in Figure 2b. In the absence of input (black solid line), there are two coexisting attractor states, an "off" state at a low level of activation and an "on" state at a high level of activation. The activation dynamics is bistable. The two attractors are separated by an unstable stationary state (zero crossing of rate of change with positive slope). Whenever initial activation is smaller than the level corresponding to this intermediate state, the "off" state is reached in time. When activation is larger than the level of the intermediate state, activation grows until it reaches the "on" state.

[1] Note that the terms *excitation* and *inhibition* are not fundamental to describe the activation dynamics. Although they may be used to indicate the direction of change of the activation level (increasing for excitation; decreasing for inhibition), particular terms of the equation do not necessarily have a unique excitatory or inhibitory effect. In particular, the relaxational term, $-u$, acts as a source of excitation if activation is below zero and as a source of inhibition if it is above zero.

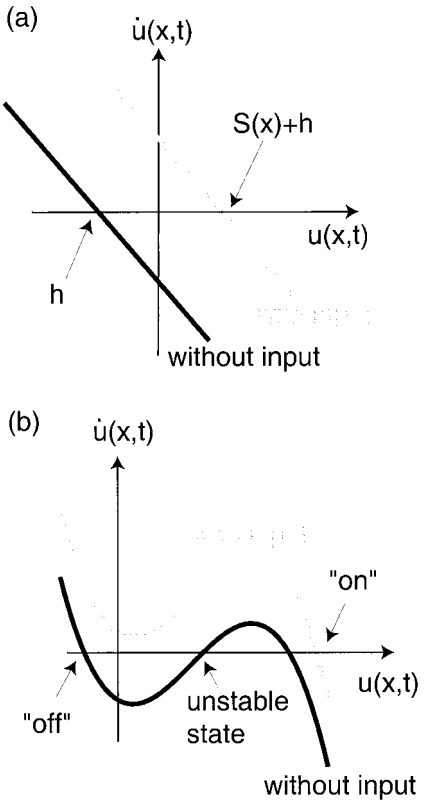

Figure 2. The rate of change of activation, $\dot{u}(x, t)$, is plotted as a function of the current level of activation, $u(x, t)$. (a) Two situations of the linear model in Equation 2 with and without input. The zero crossings of the rate of change—at the resting level, h, without input and at $S(x) + h$ with input—represent attractor states, to which the system converges in time. The negative slope of the rate of change at these zero crossings illustrates the attractor mechanism: At higher levels of activation, negative rates of change lead to decrease of activation; at lower levels of activation positive rates of change lead to increase of activation. (b) Strongly nonlinear activation dynamics. Without input there are two attractor states, one at a low level of activation ("off"), another at a high level of activation ("on"). When input is added, a single attractor state ("on") remains. The "off" state has disappeared. If input were increased gradually, this change would be characterized as an instability, in which the "off" attractor collides with an unstable stationary state.

Input acts as an additive force, lifting the rate of change across all levels of activation. At sufficient input strength (see Figure 2b), the "off" state disappears! It collides with the intermediate, unstable state, and the two dissolve, leaving no zero crossings at low levels of activation. This instability leaves the system in a monostable situation, in which only the activated state, shifted somewhat from its level without input, remains. If the system was initially in the "off" state, it now relaxes toward the activated state. When input is removed, the system returns to its bistable layout. However, if input was present for a sufficient amount of time, so that activation came sufficiently close to the activated state, it now self-stabilizes at the activated level, not returning to the "off" state. Thus, stimulation may trigger the generation of self-stabilized patterns of activation, even when stimulation is only transient.

Mapping "off" and "on" states of the activation field onto two qualitatively distinct (because coexisting) attractors of a strongly nonlinear dynamic system has important implications when we now consider how different sites of the field are interdependent. This interdependence becomes most visible when we look at a situation in which input no longer specifies uniquely a particular motor act, so that multiple field sites are activated. This may happen, for instance, because different sources of input are in disaccord, because the information from a single source of input is ambiguous or because the environment does not completely specify an action (such as when two graspable objects are in view). The activation field must either average such ambiguous information or make a decision in which only one region of the field attains the "on" state and other stimulated regions remain in the "off" state. We postulate that such decision making occurs when the stimulated sites are sufficiently far from each other. This is illustrated in Figure 3, in which input localized at two locations of the field leads to an activation pattern in which a single peak of "on" state activation is stabilized at one of the two locations. At which of the two specified locations this peak is positioned may depend on chance, on prior activation in the field (the prior history of activation), or on slight asymmetries in the input pattern (for modeling and discussion of such decision making in the context of the preparation of saccadic eye movements, see Kopecz & Schöner, 1995).

This capacity of the field to stabilize decisions in the face of ambiguous input information is brought about by interactions within the field. Interactions are dependencies of the rate of change at one location, x, on the activation at other sites, x', of the field.

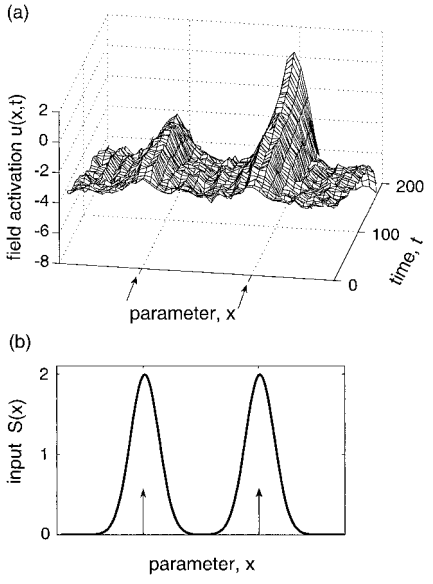

Figure 3. The dynamic field (a) may generate a single localized peak of activation in response to bimodal input (b). Input localized at two sites (arrows) is applied at time $t = 0$. The field initially develops two peaks of activation, which inhibit each other. Fluctuations enable the right-most peak to win the competition. A decision to activate the left-most site instead would have been possible as well (bistability). Strong interaction thus endows the field with the capacity to make "decisions" in the face of ambiguous input.

The interaction needed here is one that leads to strong nonlinearity of the field dynamics (cf. Equation 3 and Figure 2b). Consider, for instance, a bimodal pattern of input, illustrated in Figure 3. Decision making means that although two sites receive appropriate input, activation reaches an "on" state only at one site, remaining in the "off" state at the other. Because either site could be selected, the overall dynamics is bistable (but now in the presence of input!). Thus, a one-to-one link between input and activation pattern no longer exists.

There is no unique mathematical formulation for such "strong" interactions (Amari & Arbib, 1977; for a related conceptualization of decision making in terms of competitive dynamics, see Grossberg, 1980). Qualitatively, the following assumptions constrain the ideas: First, we assume that only those sites in the field contribute to interaction that are sufficiently activated. Mathematically, this is the origin of strong nonlinearity and can be expressed through a sigmoid function (see Figure 4a; Grossberg, 1973). Second, we assume that the field varies smoothly along the movement parameter dimension, *x*. This can be guaranteed by having neighboring sites provide positive input to each other (local excitation; see Figure 4, b and c). Third, we assume that field sites compete when they are sufficiently far from each other. Competition means that the sites provide negative input to each other (global inhibition; see Figure 4, b and c).

For our modeling we have adopted a particular mathematical form of such an interacting field dynamics, first analyzed by Amari (1977):

$$\tau \dot{u}(x, t) = -u(x, t) + S(x, t) + h + \int w(x - x')f[u(x', t)]dx'. \quad (4)$$

The sigmoidal function, $f(u)$, and the interaction kernel, $w(\Delta x)$, are illustrated in Figure 4, a and b, and given in more detail in Appendix A. Integration over the entire field collects input from all activated regions of the field, which acts as positive input when originating from the vicinity of the site, *x*, and as negative input when originating from regions further removed from *x*. The mathematical properties of this particular formulation are reviewed in Appendix A. Compared with other, related formulations (Grossberg, 1973; Wilson & Cowan, 1973), the Amari equation has the particular advantage that rather complete mathematical analysis is possible, which helps establish a clear theory–experiment relationship by making the choice of parameter values transparent.

Because bistability and instabilities play an important role in this formulation, there are situations in which minor changes of activation may push the system either toward the "on" or toward the "off" state. Therefore, random perturbations from other processes, from sensory input, or from the motor system must be taken into account. Such perturbations are modeled as stochastic inputs (cf. Appendix A), so that the activation field as a whole is an ensemble of dynamic stochastic processes.

Dynamic Field Model of Movement Preparation

How can these concepts be used to model the process of specification of a movement parameter? To be concrete, we continue to refer to the parameter of movement direction, *x*, represented by a dynamic field that evolves under the influence of two sources of inputs, specific and task input (see Equation 4 and Figure 5).

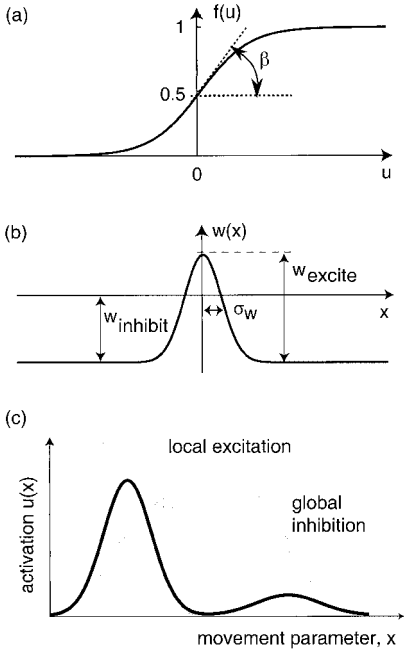

Figure 4. (a) Each location contributes to interaction only to the extent that its local activation exceeds a soft threshold, modeled as a sigmoid function, $f(u)$. The slope, β, of this function determines the degree to which subthreshold values of activation (smaller than zero) contribute to the interaction. This affects the effective spatial range of interaction as well. (b) Interactions in the field are modeled by an interaction kernel $w(x)$ with a local excitatory zone of width σ_w and strength w_{excite} and a global inhibitory contribution of strength w_{inhibit}. (c) Schematic of the interactions involved in generating a localized peak of activation (black line) in response to bimodal input (gray line; cf. Figure 3). Once the left-most peak of activation is sufficiently strong, it is supported by local excitatory interactions and suppresses activation at the right-most site through global inhibitory interaction. By contrast, activation at the right-most site is capable neither of locally "self"-exciting nor of inhibiting the left-most site, because the sigmoid nonlinearity suppresses its contribution to interaction. The initial advantage of one site may come about because of stronger input (as hinted here) but may also be due to fluctuations or the prior history of activation.

Specific Input

The sensory processes that provide the field with specific information about the upcoming movement are modeled by a pattern of input activation, $S_{\text{spec}}(x, t)$. For example, visual information may specify a single location in the field, which is represented by an input pattern with a single peak located at the specified location. Multiple sources of sensory specification may contribute to this input, including learned stimulus–response associations and channels of automatic activation (Kornblum, Hasbroucq, & Osman, 1990). We define those sources of specification as *specific input*, which is provided at a particular point in time, subsequent to which the movement is performed. In experiments, such specification is

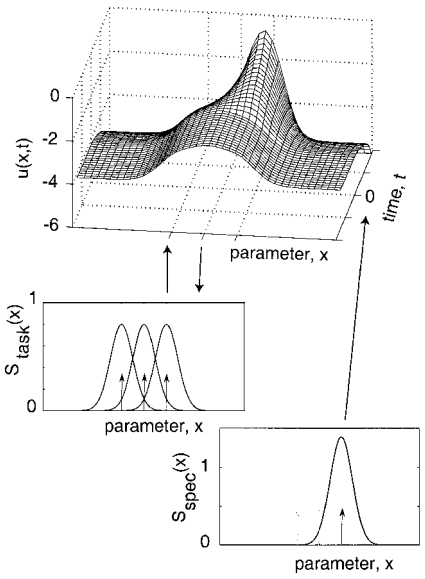

Figure 5. The movement parameter field, $u(x, t)$ (top), evolves in time under the influence of two inputs. The task input (S_{task}, bottom left) represents the task environment and is present before the sensory signal that triggers movement preparation on any particular trial. Here, three overlapping preshaping contributions represent three values of the movement parameter (indicated by three arrows) relevant in the task. The metrics of these three choices lead in the example to a broad, monomodal activation peak centered on the three parameter values, observable as the "preshape" of the field at early times. The specific input (S_{spec}, bottom right) represents sensory information that specifies the upcoming movement and is present only after the corresponding signal is provided (here at time $t = 0$). The specific input triggers the growth of a single localized peak of activation that attains enough strength to self-sustain and thus to suppress activation at other sites. Ultimately, the self-sustained peak is therefore positioned over the parameter value specified by the specific input and is little affected by the task input. The input strength for the specific input, g_{spec}, was 1.4, and the input strength for the task input, g_{task}, was 0.8. When the dynamics of the memory field is modeled at a slower time scale, then that field is reciprocally coupled with the movement parameter field evolving on a slower time scale, which leads to reciprocal coupling from the movement parameter field into the memory field.

often provided jointly with a go signal. In the model, specific input is then assumed to abruptly arise at that point in time.

Task Input

When the sensory signal specifying a motor act arrives, this signal does not encounter a totally unprepared system. The field is never a tabula rasa but rather is always prestructured to reflect whatever is available as prior information about the upcoming motor task. There are multiple ways in which such prior information can become available. First, the perceptual layout of the task may suggest only a limited number of motor acts (for instance, when a limited number of graspable objects or pressable buttons are in the work space). Second, individuals might understand the task and intentionally prepare particular motor acts. Third, movements prepared previously may leave a memory trace that preactivates the field. Below and in Appendix B we propose a dynamic field model of how such memory traces are formed. Finally, prior information about the upcoming movement task, precued ahead of the final response signal (Rosenbaum, 1980), may prestructure the field.

Such prestructuring of the field is modeled by assuming that a second source of input, the *task input*, is available. Like specific input, task input represents information through its spatial structure (see Figure 5). For instance, a broad localized peak of task input may represent a set of closely spaced parameter values over which it is centered. We assume that task input is present before specific input arrives. Thus, the field has relaxed to the stable state determined by task input (the field is "preshaped" by task input) at the time when specific input is supplied.

Results for One-Dimensional Model

We study the processes of movement preparation in two settings, the timed movement initiation paradigm and the reaction time paradigm.

Timed Movement Initiation

Imagine you are a goalkeeper in soccer or handball confronted with a player executing a penalty kick or throw. If you start moving toward the ball only once clear sensory information is available about the trajectory of the ball, you might come too late to intercept it. Skilled goalkeepers are known to initiate movement very early, often with incomplete specification of movement direction. They "guess" the corner. Many other action–perception tasks require that initiation of a movement be timed to perceived events (for a review, see Lee & Young, 1986).

A laboratory version of this scenario is the timed movement initiation paradigm, developed by Ghez and colleagues (Ghez et al., 1990; see also earlier work by Schouten & Bekker, 1967). Participants are trained to initiate a movement (or, in some experiments, an isometric force pulse) at a particular point in an external metronome sequence (e.g., on the fourth tone of an auditory metronome). Which movement must be performed is specified at a particular time before that imperative signal. The time interval between the signal that specifies the movement and the metronome signal that triggers initiation of movement (the stimulus–response interval) is varied from trial to trial. When this interval is sufficiently long, the movement can be prepared beforehand. When this interval is short, there is little time available to prepare the movement, so the movement parameter value must be guessed.

As a first example, consider the experiment of Hening, Vicario, and Ghez (1988). Participants produced isometric force pulses whose amplitude had to match one of three target amplitudes. In Figure 6 we have redrawn a part of their experimental results. Stimulus–response intervals were binned into three groups. Histograms of the actual peak force generated by participants are shown separately for the cases when either the medium or the smallest level of force was required. For the shortest stimulus–response intervals, an initial "default" distribution was centered over the average of the three required peak forces irrespective of which force level was specified. This distribution was considerably narrower than the total range of required forces. The distributions evolved continuously for increasing stimulus–response intervals. When the smallest or largest level of force was specified, the distributions shifted gradually until they were centered on the

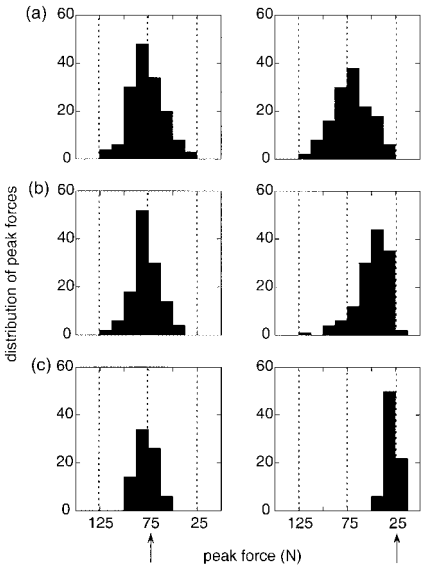

Figure 6. Experimental data from Hening, Favilla, and Ghez (1988, Figure 5c) were used to generate this figure. These authors measured the isometric force pulse amplitude generated in a timed response paradigm with three equally probable target amplitudes (dashed lines). Histograms of peak generated forces are shown based on responses in three intervals of stimulus–response time: (a) early, stimulus–response interval $<$ 125 ms; (b) middle, 125 ms $<$ stimulus–response interval $<$ 250 ms; and (c) late, stimulus–response interval $>$ 250 ms). The left column refers to the condition in which the medium force level (indicated by the arrow) was specified and the right column to the condition in which the smallest force level (indicated by the arrow) was specified.

specified force level for the largest stimulus–response intervals. During this shift, the distributions were centered at levels of force that were never specified. The shifting distributions transiently broadened. In all cases, the distributions eventually sharpened compared with the initial state.

The observation of an early default distribution implies a bias toward the center of the range of possible force amplitudes. This early bias was a range effect rather than an effect of absolute scale: When the absolute scale of the three force amplitudes was varied, early responses were always biased toward the center of the three values (Hening, Vicario, & Ghez, 1988).

To model this experimental situation, we recognize that the force pulse amplitude, x, is the relevant movement parameter distinguishing the three choices. We assume that the one-dimensional activation field, $u(x, t)$, representing the movement parameter is preshaped with a broad activation peak centered on the three choices (see Figure 5). The response signal, which specifies one of the three targets, is modeled as specific input centered on the specified level of force. From the moment this input is applied, the field evolves continuously from its preshaped form to a form centered on the specified parameter value. *Continuously* refers both to the level of activation, which rises gradually, and to the position of the peak of the localized distribution of activation, which shifts gradually from its default position centered over the average of the three target directions to its specified position.[2]

The stimulus–response interval defines the time during the evolution of the movement parameter field at which the state of the field is "read out" and movement is initiated. We assume that at this time, the location with maximal activation in the field determines which movement is being realized.[3] Because the field as a whole not only evolves under the influence of deterministic inputs and interactions but is also affected by stochastic inputs and thus fluctuates, the exact location of this maximum is a random variable (see Figure 7). Its statistics can be determined by sampling across many repetitions of the same motor act. Histograms of the locations of the activation peak can be used to estimate the distribution of this random variable. Figure 8 shows such histograms obtained at four different stimulus–response intervals from a large number of repeated simulation runs. Note that the spatial shape of the histograms (see Figure 8) reflects the shape of the underlying activation field (see Figure 7).

On the basis of these stochastic parameter distributions, we can compare the model (see Figure 8) directly to the experiments of Hening, Vicario, and Ghez (1988; see Figure 6). The results match closely in terms of (a) the common and narrow initial default distribution reflecting a range effect, (b) the continuous evolution and gradual shift of the parameter distributions, and (c) their transient broadening and eventual sharpening.

What happens if the two choices are farther apart in the field? Ghez's group (Favilla, Gordon, Ghilardi, & Ghez, 1990; Ghez et al., 1997) has performed a series of experiments that probed how the metrics of the movement choices affect the parameter distributions observed in the timed movement initiation paradigm. Participants had to point at targets specified via a computer screen. In each block of trials, only two choices were relevant. In different conditions, not only the amplitude of the pointing movements but also the movement directions, on which we focus now, were varied. There were five series in which the two possible directions of movement from a common starting point were either 30°, 60°, 90°, 120°, or 150° apart. The same histogram technique as in the earlier experiment was used in observing the temporal evolution of the distributions of movement direction. For 30° and 60° of separation, early responses were distributed monomodally. These distributions then shifted gradually to the specified side for increasing stimulus–response interval. An angular separation of 60° represented approximately the crossover point, at which the initial distributions started to have a broader base, becoming bimodal beyond 60°. Bimodal distributions changed in time to monomodal, typically within about 80 ms. Whereas for narrow angular separations between movement directions the responses showed graded

[2] A subtle question is that of whether task input is removed once specific input has been applied. If task input persists throughout, the many effects described here are strong and easily obtained. We have assumed, however, that task input is removed when specific input is applied. The effects persist because of the lingering preactivation. Keeping task input "on" tends to generate more bias toward the preshaped states than is realistic. Specific input could be viewed as providing not only excitatory input to the parameter value specified but also inhibitory input to the parameter values not specified. That would, in effect, cancel task input.

[3] This can be viewed as the limit case, in which an active process of movement initiation lowers the threshold of the trajectory formation system sufficiently fast, so that movement is initiated independent of the level of activation in the field.

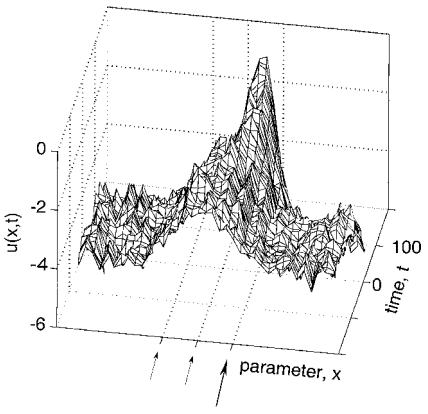

Figure 7. The evolution of the field dynamics illustrated in Figure 5 is shown with stochastic forces as an additional contribution. This stochastic dynamics generates fluctuations of activation overlaid over the deterministic time course of the field. The location of maximal activation in the field is now a random variable, as is the time when a particular level of activation is reached. The noise strength was $q = 8$; $u(x, t)$ represents level of activation. The arrows indicate the three possible values of the movement parameter. The longer arrow marks the value specified in this simulation.

bias toward an averaged direction up until about 200 ms, the wide conditions led to responses that were biased only at short stimulus–response intervals and were then narrowly focused on one of the two required directions.

Figure 9 shows histograms obtained from a set of simulations in which the metrical distance between two target parameters was varied. These results match the experiments (Favilla, Gordon, Ghilardi, & Ghez, 1990; Ghez et al., 1997) closely. First, the initial distribution is monomodal for narrowly spaced and bimodal for more widely spaced target parameter values. (This crossover can be used to estimate the width of the task input in the model; see Appendix C). Second, when the initial distribution is bimodal, a transition to monomodal occurs in time as probability mass is shifted from one peak to the other. This reflects the relaxation process of the movement parameter field, in which activation at the specified site is enhanced through specific input, which in turn suppresses activation at the other site through intrafield inhibition. Third, bias toward the mean of two parameter values is observed strongly for the narrow condition, less so for the wide condition.

The theoretical account provided by the dynamic field model shows that discrete and continuous modes of movement planning, discussed by Ghez and colleagues (Ghez et al., 1997), emerge from a single underlying mechanism. In a recent extension of these results, Favilla (1997) varied the angular separations between four possible movement directions, arranged in two groups with narrow angular separation between the two elements of each group and varied angular separation between the groups. The initial distribution of movement direction was bimodal for the widely separated groups, with each mode centered on the average direction within groups, and was monomodal for the narrowly separated groups, centered on the overall average movement direction. This flexible change from discrete to continuous movement mode of preparation emerges, of course, from our model in the same way as shown here. The shape of the initial distribution results from the metrics of the task environment relative to the intrinsic spread of task input.

We mentioned earlier that information about possible movements expressed by the task input may come from a number of sources including the perceptual layout of the work space, precues, or intentional preselection of a movement. We now focus on one factor, the recent motor history. We assume that over multiple motor acts a memory trace of the activation patterns in the movement parameter field is accumulated. On any given trial, this memory trace provides task input to the movement parameter field.

A dynamic model of the motor memory trace is based on a second field of activation, the memory field, $u_{\mathrm{mem}}(x, t)$. This field receives input from those sites of the movement parameter field, $u(x, t)$, that are sufficiently activated. Conversely, the memory field acts as task input into the movement parameter field, so that the two fields are mutually coupled (see Figure 5). Two additional assumptions constrain the mathematical modeling (details are given in Appendix B). First, the memory field is endowed with two different time scales, one effective in the presence of input from the movement parameter field, the other in the absence of such input. In the presence of input from the movement parameter field, the time scale of the memory field is longer than that of the movement parameter field, so that the memory field changes little during an individual trial but evolves over several trials. In the absence of input from the movement parameter field, the memory field decays spontaneously, but on an even longer time scale. Therefore, the memory field does not decay appreciably in the intervals between trials, and the memory trace depends little on the length of these intervals. (Mathematically, this amounts to a shunt-

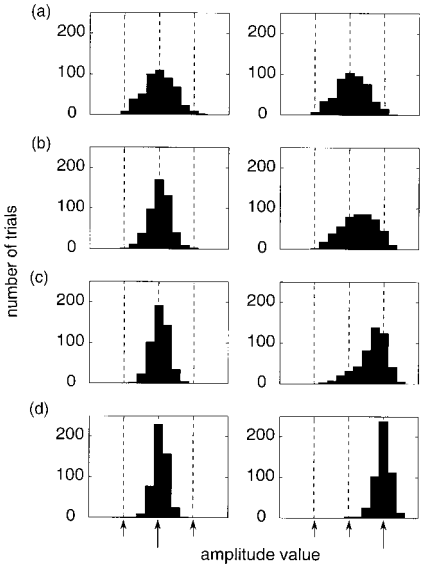

Figure 8. Histograms of read-out movement parameter values in the timed movement initiation paradigm are obtained from an ensemble of 500 simulations of the stochastic field dynamics illustrated in Figure 7. The field location with highest activation is read out in each case at four different times after application of specific input: (a) $t = 0$, (b) $t = 100$, (c) $t = 200$, and (d) $t = 300$ ms. The three parameter values specified by preshaping input are indicated by three arrows at the parameter axis and by the dashed lines, the longer arrow pointing at the parameter value specified by specific input at time $t = 0$.

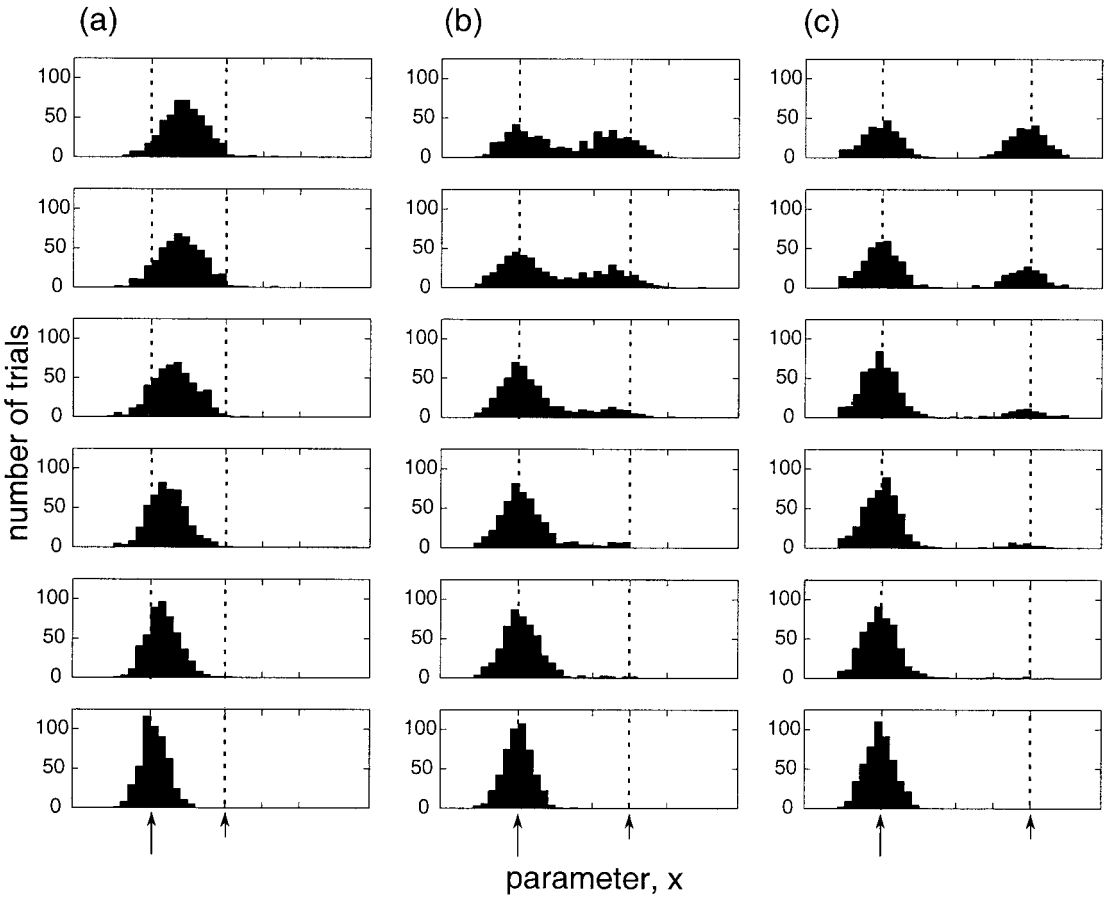

Figure 9. Three different task metrics are looked at in the timed movement initiation paradigm (times $t = 0$, 20, 50, 80, 120, and 300 ms, from top to bottom). In each case, two target parameter values (indicated by the two arrows at the parameter axis and the dashed lines) are possible, but they are spaced close to each other (a), at an intermediate distance (b), or far from each other (c). In all three cases, the left-most target (indicated by the longer arrow) is specified at time $t = 0$. (a) For closely spaced choices the shape of the distribution is monomodal at all times, with a gradual shift from an intermediate location to the correct location. This replicates the simulation of Figure 8. (b) At intermediate distances a broad, initially bimodal distribution flows toward a monomodal distribution. Early during the specificational process, metrical effects are observed as bias toward the other possible parameter value. (c) At large separation an initially bimodal distribution changes into a monomodal distribution, the peak of which is positioned correctly from the outset. The input strength for the specific input, g_{spec}, was 1.4, and the input strength for the task input, g_{task}, was 0.8.

ing mechanism of the kind introduced by Grossberg, 1973; Sperling & Sondhi, 1968.) The second assumption is to postulate that the memory field has the same form of interaction as the movement parameter field so that memory traces accumulated at different sites within the field compete with each other. This competition is weak—that is, the memory field does not make decisions in the sense discussed earlier.

The influence of the recent motor history on movement preparation is probed by the classical experimental paradigm in which the probability of the different choices is manipulated. Figure 10 illustrates how the dynamics of the memory field evolves in such a probabilistic paradigm. The preshape field is initially at a low level of activation. Over a series of trials, two movement directions are specified with different probabilities. The level of activation in the preshape field at the two sites representing the two choices evolves gradually, reaching different stationary levels of activation. Thus, the probability of each choice is represented by the amount of activation in the preshape field at the corresponding site. This representation results from a dynamic equilibrium between recurrent input to the memory field from the movement parameter field and the mutual competition within the memory field. Thus, if the probabilities of the two choices are changed, the preshape field adjusts to this changed pattern of movement history (second half of the simulation).

How does such asymmetric task input representing different choice probabilities affect performance in the timed movement initiation paradigm? In Figure 11 two sets of simulations illustrate performance when the more probable (Figure 11b) and when the less probable (Figure 11a) choice is specified. The initial distribution is monomodal, centered almost perfectly on the more probable

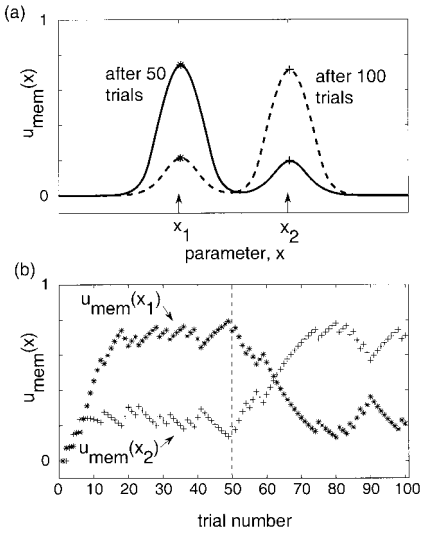

Figure 10. The dynamics of the preshape field is illustrated in a paradigm in which two target parameter values occur with different probabilities. In (a) the distribution of activation in the memory field, $u_{mem}(x)$, is shown at two points in time, after 50 trials (solid line) and after 100 trials (dashed line). The arrows indicate the two possible parameter values. In (b) the amount of activation in the memory field at the two target locations (marked by an asterisk for target x_1 and a plus sign for target x_2) is tracked over a sequence of trials. The activation at the end of each stimulation period, ΔT, is shown. During the first 50 trials, target x_1 occurred more frequently by a factor of about 3:1 (based on a pseudorandom series). During the second 50 trials, the probability ratio was inverted. Activation in the memory field relaxes from the initial zero activation state to a pattern in which target value x_1 is favored. After the switch, the activity pattern adjusts within a few trials to the new target statistics (compare activity at x_1 and x_2 after Trial 70).

choice (top panel in both columns of Figure 11). Thus, when the more probable choice is specified, the distribution of movement parameter values remains in place but sharpens in time. When the less probable choice is specified, the initial pattern of activation is centered on the wrong location. Specific input leads to growth of activation at the correct location, although that growth is slowed by inhibition from the preactivated site. The histograms are initially biased toward the more probable choice.

One aspect of these simulations can be compared with experiments reported in Favilla, Gordon, Hening, and Ghez (1990). Participants emitted isometric force pulses of two different amplitudes. Using the timed response initiation technique, the experimenters imposed a single stimulus–response interval of about 112 ms, clearly shorter than typical reaction times. The two amplitudes occurred with different probability in some conditions and with equal probability in other conditions. A clear bias of the performed amplitude toward the more probable amplitude value was observed in the conditions with unequal probability.

Other aspects of the simulations are open to test. First, the default distribution is asymmetrical. This should be observable in the timed movement initiation paradigm at small stimulus–response intervals, in particular, if the less probable choices are specified. Second, comparable precision is reached earlier when more probable targets are selected than when less probable targets are selected. Third, when the less probable target is specified, the parameter distribution evolves more slowly with gradual decay of bias toward the more probable target. Fourth, at sufficiently large metrical separation of the two choices, the temporal evolution of the parameter distribution goes through a bimodal regime when the less probable target is specified. Fifth, the more different the probabilities of the two choices, the more pronounced the bias effect and the more different the time courses of specification for the more and less probable target.

Reaction Time Paradigm

In reaction time paradigms, participants are asked to initiate movement as early as possible subsequent to a go signal that may also convey information about which movement must be performed. The urgency of the response is counteracted by a requirement to be precise (the well-known speed–accuracy trade-off). Because the time of movement initiation is thus determined by the extent to which a correct movement has been prepared, rather than by an external timing signal, we conceive of this paradigm as one in which the time of movement initiation depends on the pattern of

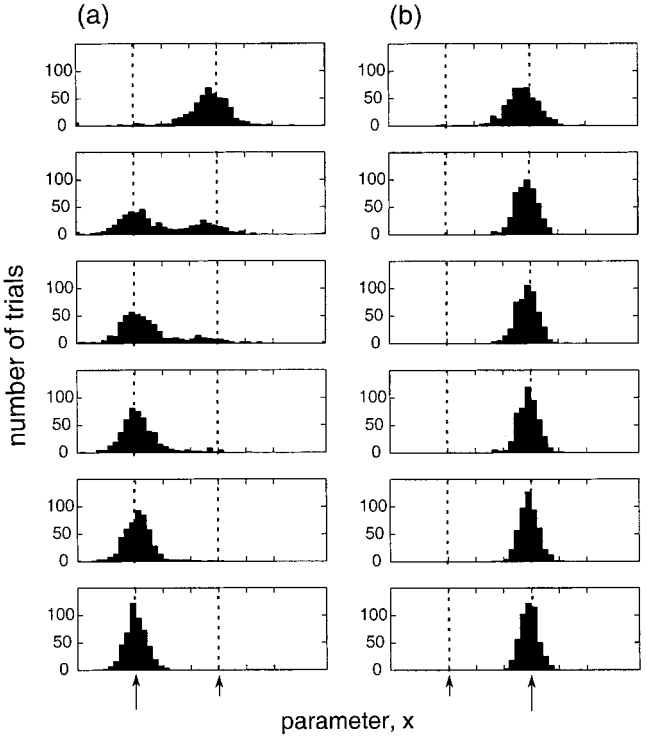

Figure 11. A task environment in which two targets occur with different probabilities is simulated. (a) The left-most (less probable) target is selected. (b) The right-most (more probable) target is selected. Histograms are shown for times t = 0, 70, 90, 120, 150, and 300 ms (from top to bottom). The preshape underlying the initial distribution is illustrated in Figure 18b on top. In both columns, the two possible movement parameter values are marked by arrows and dashed lines, the longer arrow indicating which value was specified at time t = 0. The input strengths were adjusted as follows: The input strength for the specific input, g_{spec}, was 1.2, and the input strength for the task input, g_{task}, was 0.6 and 0.2 for the more and less probable target, respectively.

activation in the movement parameter field. As a simple description, we use the standard idea of a threshold: When activation in the movement parameter field first exceeds a threshold level, a movement is initiated. The movement is characterized by the parameter value that corresponds to the point in the field at which the threshold was pierced.

Because of the random fluctuations of the activation field, the threshold is reached at randomly different times and randomly different parameter values in repeated trials. By accumulating statistics over such trials, one can estimate the stochastic properties of the two random variables, movement initiation time and movement parameter value. These movement initiation times, counted from the moment in time when the specific input was applied, are interpreted as a measure of the contribution of movement preparation to reaction time.

Preshaping Affects Reaction Time

Metrics of choices. The general idea of how the preshaping of the movement parameter field affects reaction time is this: The more similar the preshaped pattern of activation is to the specified pattern, the faster the field reaches threshold (short reaction times) and the more likely it is that it reaches threshold at the right location (few errors).

One way the similarity between preshape and specified patterns can be varied is by the spatial layout of the task. When the different possible movements are closer to each other, specifying any one of them involves more similar patterns than when the different movements are more dissimilar. This leads to the surprising and counterintuitive prediction that reaction time is shorter when one of a set of more similar movements is specified than when one of a set of more distinct movements is specified. Were the preparation of a movement viewed as a discrimination task, in which the specified movement has to be recognized as different from the other possible movements, then the opposite would be expected. Perceptual judgments, for instance, are classically known to require longer reaction times when the stimuli are more similar to each other (Johnson, 1939).

Surprisingly, the effect of response metrics on reaction time has not been much studied. When one of us (Gregor Schöner) moved to Marseille, France, with most of dynamic field theory developed, he learned from the late Jean Requin (personal communication, 1994) about an early experiment that directly addressed the effect of task metrics. Published in French (Fiori, Semjen, & Requin, 1974), this result has remained largely unnoticed. In the experiment, participants pointed toward one of two possible targets as specified by a highly compatible light display. In different blocks of trials, the two targets were arranged spatially such as to require pointing movements with different angular separations. The angular distance between the directions of the two pointing movements significantly affected reaction time, which increased from 45° of angular separation to 135° and dipped again slightly for a separation of 180°. A study by Bock and Arnold (1992) showed that increasing the range of expected movement directions (or amplitudes) increased reaction time, which is consistent with the metrical effect but could also be attributed to the different amounts of stimulus uncertainty in the different conditions.

In the model, we simulated a two-choice reaction time task in which the metrical distance between the two movement parameter values is varied (see Figure 12). The specific input induces a peak at one of the two locations (the left-most choice). Activation rises earlier, leading to shorter reaction time, the more similar the two movement directions are to each other. In the model, this effect is due to the gradual shift from overlapping excitatory input to primarily inhibitory interaction as the metrical distance between choices increases. As a corollary, we observe that bimodal preshapes (here assumed at angular separations of 90° and 135°), in which inhibition dominates, lead to delayed buildup of activation compared with monomodal preshapes (here assumed at angular separations of 45° and 60°).

The performed movements are also affected by the metrics of preshape. Similar to what occurs in the timed movement initiation paradigm, the distribution of performed movement parameter values may reflect the shape of the underlying dynamic field. This will be true only if movement is initiated early in the process of movement preparation. Experimentally, emphasizing urgency over accuracy produces such conditions.

In the model, the threshold level at which movement is assumed to be initiated can be used to model degrees of urgency. In Figure 13, three different levels of threshold are applied in a three-choice reaction time task with monomodal preshape (the same condition as first shown in Figure 5). At low levels of

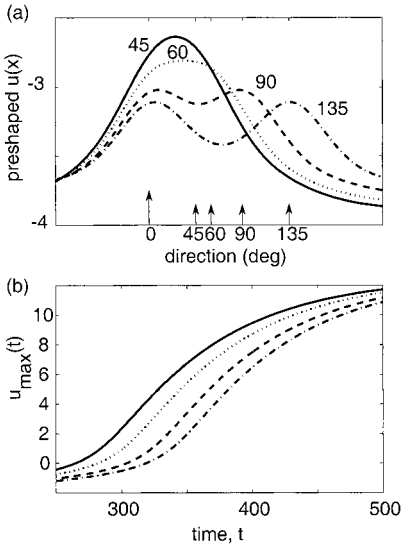

Figure 12. The effect of the metrics of choice on reaction time illustrated through individual simulations of a dynamic field representing movement direction. (a) The preshaped pattern of activation representing two-choice tasks at four different angular separations between the two possible movement directions (45°, 60°, 90°, and 135°; deg = degrees). At time $t = 0$, specific input specifies the shared movement direction at 0 (longer arrow). The shorter arrows indicate the second possible movement direction in the different conditions. (b) The maximal level of activation in the field, $u_{max}(t)$, is plotted as a function of time (in milliseconds) for the four conditions; line types match those in (a). Activation rises earlier, the more closely spaced the two movement directions. This effect is observed even when the two bimodal preshapes are compared (90° and 135° of separation). Parameters were chosen as follows: The input strength for the specific input, g_{spec}, was 1.4; the input strength for the task input, g_{task}, was 0.4; the width of the local excitatory zone, σ_w, was 20; and the strength of the local excitatory zone, w_{excite}, was 1.6.

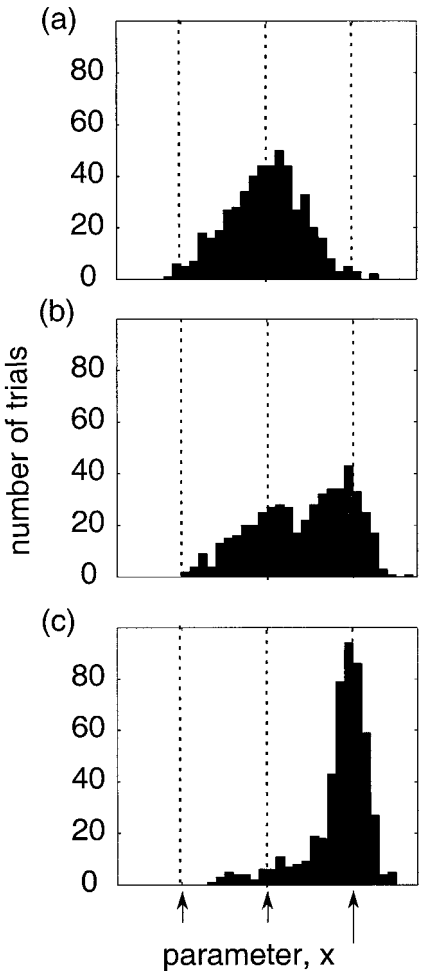

Figure 13. The simulations illustrated in Figure 5 are now analyzed in the reaction time paradigm. Of the three possible parameter values (arrows and dashed lines), the right-most (longer arrow) value is specified at time $t = 0$. The location at which field activation first reaches a threshold level is recorded in each trial out of an ensemble of 500 simulations. Histograms of those locations are shown for three different threshold levels: (a) −2.0, (b) −1.4, and (c) −1.0. Note strong range effects at low thresholds, that is, (a) and (b): Values are biased toward the mean of the three movement parameter values.

threshold (urgency emphasized; see Figure 13, a and b), the preshape is strongly visible in the distributions of performed movement parameter values, which are centered over the range of possible movements. This is because low levels of threshold lead to shorter reaction times, at which the preshape continues to affect the shape of the dynamic field. This understanding leads to a prediction: At fixed threshold, movements performed on trials with short reaction times reflect task input by being biased toward the center of the range of possible movements, whereas movements on trials with larger reaction times reflect primarily specific input and have little bias. Figure 14 illustrates this predicted pattern of results. The data obtained at intermediate threshold from the previous figure were divided into two halves, grouping the faster and the slower reaction times. The faster trials have a parameter distribution closely matching task input, whereas the slower trials have a distribution centered on the specified target. The influence of preshape on the metrics of performed movements thus provides an account for the range effects known to occur under conditions of urgency (Hening, Vicario, & Ghez, 1988; Poulton, 1981).

Number and probability of choices. Another way the similarity between preshape and the specified pattern of activation may vary is through the number and probability of choices. Each choice defines a contribution to the task input localized around the parameter value specified by that particular choice. For large metrical distances between the different choices, the task input may induce a multimodal pattern of preactivation as illustrated in Figure 15. For more narrowly spaced choices, a broad monomodal preshape may result. In either case, the larger the number of choices, the more dissimilar the preshape from the pattern of activation induced by specific input, centered on a single choice.

As a consequence, the larger the number of choices, the more the inhibitory interaction from the more broadly distributed preshape slows the growth of activation at the specified location (see Figure 15, bottom). This leads to an account for the classical stimulus uncertainty effect, as formalized in Hick's (1952) law,

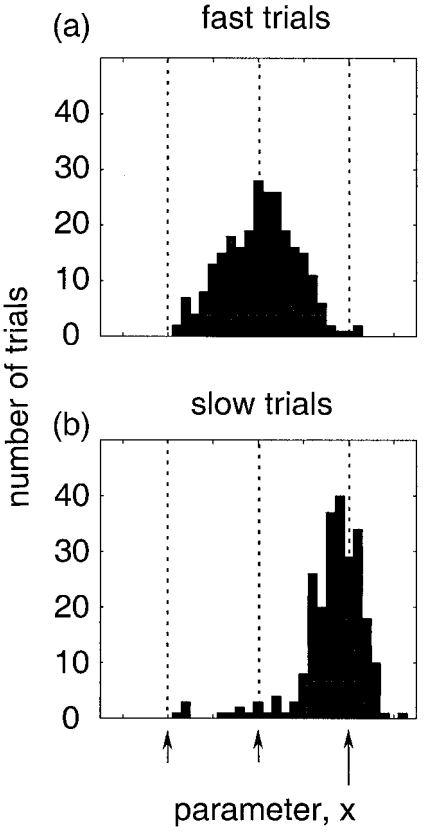

Figure 14. The trials at the intermediate threshold level (−1.4) in Figure 13 were split into two groups along the median of reaction time (time at which field first reaches threshold, $N = 250$ for each group). The figure shows the comparison of the distributions of read-out parameter values for fast (a) and slow (b) trials. Fast trials show stronger range effects than slow trials. The arrows and dashed lines indicate the three possible values of the movement parameter. The longer arrow marks the value specified at time $t = 0$.

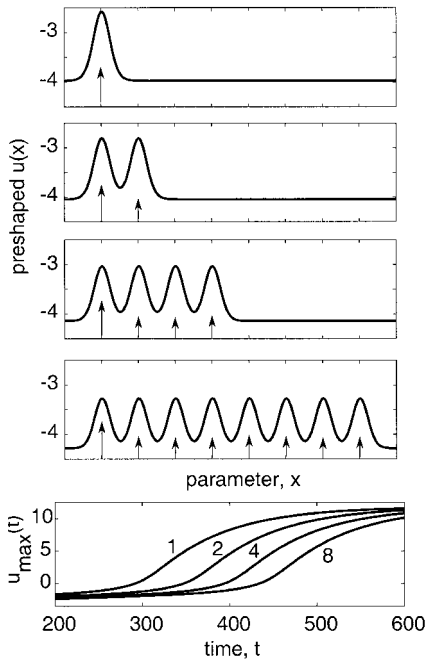

Figure 15. A demonstration of the stimulus uncertainty effect from individual simulations. The top four frames illustrate the preshaped field in task settings with (from top to bottom) one, two, four, and eight choices marked by arrows. In the bottom frame, the time courses (in milliseconds) of the maximal level of activation, $u_{max}(t)$, are shown. The left-most target (longer arrow) was specified. Activation takes longer to reach comparable levels with increasing number of choices. To accommodate the maximum number of eight nonoverlapping peaks, the total range of parameter values was extended to 450 units with corresponding kernel size (cf. Appendix C). The kernel parameters were adjusted so that the balance of excitatory and inhibitory interaction remained unchanged: $w_{inhibit} = 1.4$, $w_{excite} = 2.4$. The input strength for the specific input, g_{spec}, was 1.12, and the input strength for the task input, g_{task}, was 0.8.

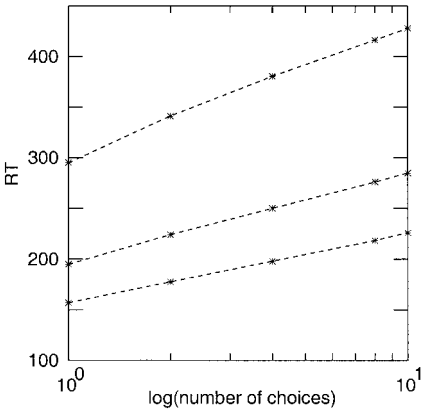

Figure 16. From simulations of the type shown in Figure 15 reaction time (RT; in milliseconds) is determined by setting the field threshold at the level of $u = 0$. The times at which this threshold is reached are plotted (asterisks are connected by lines as guides to the eye) as a function of the natural logarithm of the number of choices as in Hick's (1952) law. The three lines correspond to three different levels of strength of specific input relative to task input (the input strength for the specific input, g_{spec}, was 1.12, 1.4, and 1.6 from top to bottom), representing increasing stimulus–response compatibility.

according to which reaction time increases with increasing number of choices. In Figure 16 we assess this law quantitatively by plotting the reaction time estimated from the simulations (using a fixed threshold) as a function of the logarithm of the number of choices. Apparently, the increase of reaction time approximates the logarithmic form predicted by Hick's law but saturates slightly at larger number of choices.

This is corroborated by an analytic estimation of reaction time, shown in Figure 17 and obtained in the limit case, in which the inhibitory interaction among the different sites is independent of the metrical distance between choices (see Appendix D). This analytic estimation is helpful in understanding where both the logarithmic dependence on the number of choices and its breakdown at large number of choices come from: As the number of choices increases, the amount of activation distributed over the movement parameter field increases linearly. At constant lateral inhibition the distance in terms of total activation between the initial field distribution and the target distribution thus also increases linearly with the number of choices. The exponential relaxation law of the field dynamics then leads to a logarithmic increase in the time needed to relax to the target state, or, equivalently, to reach a threshold. Deviations from the logarithmic form are caused by self-inhibition within the preshaped field. These make the total activation in the preshape grow more slowly than linearly. As the number of choices increases, self-inhibition of the preshape accumulates until, beyond a certain critical number of choices, the preshape activation does not change further. Thus, the logarithmic law is predicted to saturate at large numbers of choices.

The probability of a choice also affects how similar the preshaped field is to the pattern induced by specific input. We had earlier shown how the dynamics of the memory field leads to patterns of task input in which highly probable movement param-

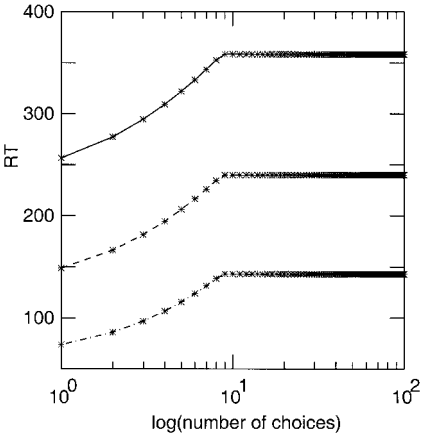

Figure 17. Hick's (1952) law as predicted from an analytic approximation in the limit case of homogeneous interaction (see Appendix D). The parameter values shown here do not exactly match those used in the simulations analyzed in Figure 16. The three lines correspond to increasing stimulus–response compatibility modeled by increasing strength of specific input, S_{spec}, from top to bottom. RT = reaction time (in milliseconds).

eter values are more preactivated than less probable movement parameters (see Figure 10). When specific input selects a probable movement, the specified pattern with a single peak at the selected location is more similar to the preshaped pattern than when specific input selects a less probable movement. As a consequence, the more probable a choice, the earlier activation builds up. This provides an account for the probabilistic version of the stimulus uncertainty effect as formalized in Hyman's (1953) law.

Figure 18 shows simulations that support this account. In all columns, the preshape, shown on top, has higher activation at the right-most, more probable parameter value. This difference of probability is smaller in Figure 18a than in Figure 18b. In both conditions, maximal activation in the field builds up earlier when the more probable choice is specified than when the less probable choice is elicited. This advantage of the more probable choice is larger for larger difference in probability. Conversely, reaction time increases with decreasing choice probability. The logarithmic relationship between probability and reaction time of Hyman (1953) is obtained in the model if probability and preshape level

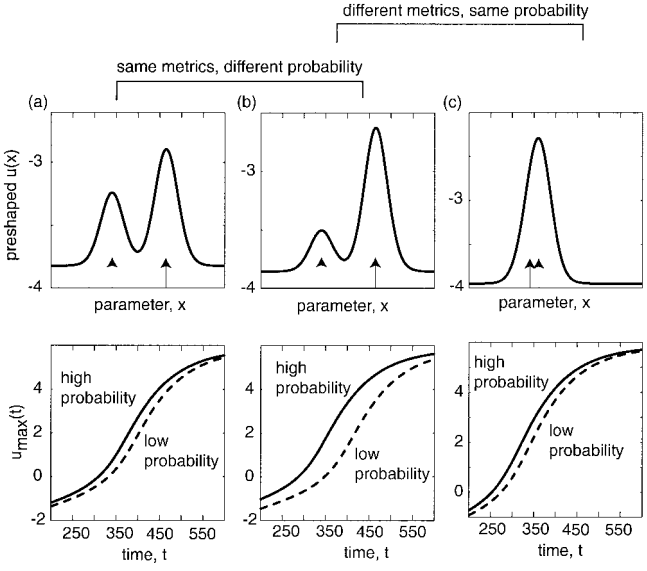

Figure 18. The effect of the probability of choices on reaction time and its interaction with the task metrics are illustrated. In each column, the preshaped field is shown on top with two arrows indicating the two parameter values relevant in a two-choice task. In all cases, the right-most parameter value is more probable and, therefore, more highly preactivated. The time course (in milliseconds) of the maximal level of activation in the field, $u_{max}(t)$, is shown on the bottom when either the more probable (solid lines) or the less probable target (dashed lines) is specified. The first two columns illustrate the effect of probability. The probability ratio is smaller in (a) (3:2, $g_{task} = 0.72, 0.48$) than in (b) (3:1, $g_{task} = 0.9, 0.3$). In both cases, activation rises earlier when the more probable choice is specified, but this difference is larger for the larger probability ratio consistent with the Hyman (1953) law. The last two columns illustrate how this effect interacts with the task metrics. The probability ratio is the same in both simulations, but the metrics of the task differ. When the task involves two narrowly spaced movements (c), activation rises earlier than when the two movements are less similar (b). The effect of probability is much reduced at close metrical distance between the movement parameters. The input strength for the specific input, g_{spec}, was 1.8 throughout.

are linearly related and the interaction between the different sites is independent of their distance in the field (see Appendix D for analysis).

The influence of probability on reaction time interacts with the metrics of the choices. The two right-most columns of Figure 18 show the comparison between conditions with identical ratio of probabilities but different metrical distance between the two movements. In both cases, the more probable choice leads to earlier rise of activation than the less probable choice. This effect of probability is much reduced, however, when the two choices are metrically closer (Figure 18c). Preactivation at the less probable sites is now increased by overlapping input from the nearby probable location as well as by excitatory interaction.

If we interpret choice probability as determining the amount of information to be processed, then this prediction implies that the amount of information to be processed is not sufficient to characterize the processes of movement preparation. The contents of the information being processed matters—that is, it matters which movements are being prepared.

Specific Input Affects Reaction Time

In the previous section we have worked with the idea that task environments preshape the movement parameter field and that the time needed to build up an adequate activation profile in the field depends on the distance between the preshaped and the required activation distribution. This distance depends, of course, not only on the preshape but also on the required activation pattern. That pattern is determined by specific input that defines the movement goal. In this section we investigate how specific input varies in different task settings and establish the implications for reaction time.

Stimulus–response compatibility. One factor that directly impacts on specific input is the degree of stimulus–response compatibility. To model stimulus–response compatibility effects, we use ideas from the dimensional overlap account (for a review, see Kornblum et al., 1990). Each source of sensory information that leads to automatic activation of a response is represented as an excitatory specific input to the field. Thus, arrangements in which multiple sources converge (high stimulus–response compatibility) are described by stronger specific input, leading to shorter reaction times (see Figure 19). Mathematically, this is due to the fact that increasing the strength of the specific input shifts the stationary state of the field to higher levels of activation (cf. Equation 2). The initial activation pattern, generated by the preshaping input, is therefore at a larger distance from this level, so that the stabilizing forces are larger, driving activation up more quickly. (See Appendix D for an approximate analytic treatment.)

Modeling stimulus–response compatibility by adding up contributions to specific input, simple as it is, leads to a very general prediction: All effects caused by the task environment decrease in size with increasing stimulus–response compatibility. This is because increasing specific input shifts the balance of inputs away from task input. Thus, preshape has a relatively smaller impact on the evolution of activation, and all effects that are due to differences in preshape are reduced in size. Reaction time depends, for instance, less sensitively on the number of stimulus–response pairs for more compatible displays. Figure 17 illustrates this prediction as obtained analytically in the approximate model detailed in

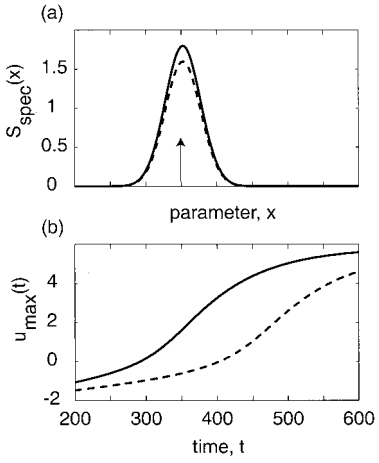

Figure 19. Modeling increasing degrees of stimulus–response compatibility by increasing strength of specific input, $S_{spec}(x)$ (a), leads to earlier rise of maximal activation, $u_{max}(t)$, in the field (b); time is given in milliseconds. Solid lines: The input strength for the specific input, g_{spec}, was 1.8. Dashed lines: The input strength for the specific input, g_{spec}, was 1.6. The arrow marks the parameter value specified at time $t = 0$.

Appendix D: The slope of the Hick–Hyman law is reduced as stimulus–response compatibility is increased. The same result is obtained from simulations of the dynamic field using different levels of specific input (Figure 16). This account is in agreement with the experimental literature (for reviews, see Fitts & Posner, 1967; Keele, 1986).

The Simon effect. If different sources of information do not converge, then specific input is supplied to multiple locations of the field. In the task setting of the Simon effect (Craft & Simon, 1970), one field site receives dominant input, all other sites being stimulated less. Although there are many versions of this classical effect (for a review, see Lu & Proctor, 1995), consider the simple setting in which a symbolic visual code specifies one of two movements. For instance, a letter *L* may indicate that the left-most of two response keys must be pressed and a letter *R* that the right-most key must be pressed. That visual stimulus may be provided in a neutral spatial position (e.g., on the midline of the visual array) or in an asymmetrical position (e.g., to the right or to the left of midline). The spatial location of the stimulus is an irrelevant dimension because it does not specify any particular movement. If the *R* signal is presented on the right, the *L* signal on the left, then the irrelevant dimension is presented in *congruent* form. If the arrangement is crossed, then the irrelevant dimension is presented in *incongruent* form. If the signal is presented in the center, then the irrelevant dimension is presented in *neutral* form (but see below for other kinds of neutral conditions). The Simon effect consists of the finding that reaction time depends on the irrelevant stimulus dimension: Reaction time is shortest when the irrelevant dimension is congruent, intermediate when it is neutral, and slowest when it is incongruent with the specified response.

How the dynamic field model accounts for this effect is illustrated in Figure 20. The complete specific input (Figure 20a) contains a small irrelevant contribution (shown in Figure 20b on a larger scale). This irrelevant contribution is assumed to arise automatically based on the spatial position of the stimulus. When the irrelevant contribution converges with the symbolic information, activation (Figure 20c) rises earlier than if it is incongruent. This is due to two factors: A congruent irrelevant contribution adds to activation at the specified sites and thus speeds the buildup of activation, and an incongruent irrelevant contribution generates activation at a competing site, which inhibits buildup of activation at the specified site.

A similar mechanism has been postulated in the discrete neural model of Zorzi and Umiltà (1995), in which a pair of neurons represents two choices and another pair the irrelevant dimension (left and right spatial position of stimulus). By embedding such an account into the dynamic field framework, we arrive at new insights, however. We predict, for instance, that the Simon effect interacts with the metrics of the task, represented in the field by the distance between activated field sites. This prediction can be derived by analyzing the neutral condition, on the basis of which *facilitatory effects* (characterized by shorter reaction times in congruent than in neutral conditions) and *interference effects* (characterized by longer reaction times in incongruent than in neutral conditions) can be distinguished. In the simulations shown in Figure 20, the neutral condition was modeled by adding an irrelevant component to specific input that was positioned symmetrically between the two choices. When these three sites are far from each other, they interact essentially only through inhibition. Thus, the neutral condition and the incongruent condition become equivalent: Both compete with the specified location. The interference component of the effect will become very small. Thus, at large

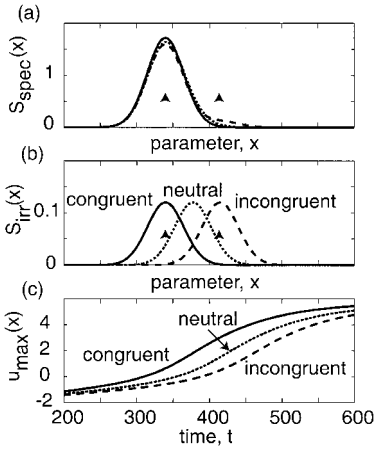

Figure 20. How the Simon effect (Craft & Simon, 1970; for a review, see Lu & Proctor, 1995) arises from the model is illustrated. The field is preshaped at the two parameter values (marked by arrows) representing the two choices. Illustrated are simulations in which the left-most target is specified. (a) Specific input, $S_{spec}(x)$, consists of a dominant contribution centered on the specified site and a smaller irrelevant contribution, $S_{irr}(x)$, illustrated in (b), centered over that same site (congruent: solid line), a symmetrical site (neutral: dotted line), or the alternate site (incongruent: dashed line). (c) Maximal activation in the field rises earliest when irrelevant input converges (solid line) and slowest when it is incongruent (dashed line); the neutral condition leads to an intermediate timing of activation buildup (dotted line); time is given in milliseconds. Task metrics affect the relative size of these effects. The input strength for the specific input, g_{spec}, was 1.6; the input strength for the task input, g_{task}, was 1.2; and the input strength for the irrelevant input, g_{irr}, was 0.12.

metrical distances between the choices, the Simon effect will show primarily a facilitatory signature. Conversely, when the three sites are very close to each other, they overlap. Irrelevant input in the neutral condition now has a facilitatory effect similar to that of irrelevant input in the congruent condition. The facilitatory component of the Simon effect thus becomes very small. The interference component is reduced as well, but less so, because the gradient of overlap is larger at larger distances from the specified location. Thus, at small metrical distances, the Simon effect will show primarily an interference signature. The interference signature is not obtained when the neutral condition consists of a stimulus that does not contain an irrelevant component (e.g., when the letter codes are presented acoustically to both ears). In the simulations of Figure 20, the task metrics were at the crossover between the two regimes, leading to an approximately symmetrical Simon effect (as much facilitation as interference when neutral is compared with congruent and incongruent conditions).

Evidence for asymmetrical Simon effects has recently been reported (e.g., Hietanen & Rämä, 1995), although there is an ongoing discussion about response strategies contributing to the observed reduced size of the interference effect (Rubichi, Nicoletti, Umiltà, & Zorzi, 2000). The role of response metrics in the Simon paradigm remains to be established experimentally.

Multidimensional Dynamic Fields: Specifying Multiple Parameters

Any motor act is characterized by more than a single parameter, including at least amplitude, direction, speed, frequency, effector, and so on. Although interdependencies may exist between some of these parameters, there is no doubt that more than one parameter can be varied by task demands. Formally, one might think of multiple parameters as spanning a higher dimensional space of parameter vectors, $(x_1, x_2, \ldots, x_n)$. The dynamic field concept could thus be generalized to multiple parameters by conceiving of a multidimensional activation field, $u(x_1, x_2, \ldots, x_n)$, so that for each location in the vector space of movement parameters an activation variable is defined.

Multidimensional Dynamic Fields

For simplicity consider only two movement parameters, (x, y), say, movement direction and amplitude. In which sense can these two parameters be said to share a single field of activation, $u(x, y)$? Are there conditions under which two separate activation variables, $u_1(x)$ and $u_2(y)$, must be postulated, each representing separately one of the two parameters?

Rosenbaum's (1980) precuing paradigm can serve to distinguish between these two cases. In the experiments, prior information is provided on each trial about one, two, or three movement parameters. For instance, a precue signal may indicate to participants that the upcoming movement has the larger of two possible amplitudes and must be performed with the right hand, leaving only the direction of the movement to be specified by the response signal. The typical outcome is that the more that is known about an upcoming movement, the shorter the reaction time. Not all parameters are equal, however. Knowing direction, for instance, reduces reaction time more than knowing amplitude. Similar differences have been documented for such parameters as the amount of resistance to overcome (Riehle, MacKay, & Requin, 1994) or the duration of the movement (Vidal, Bonnet, & Macar, 1991).

The fact that prior knowledge about any movement parameter reduces reaction time argues in favor of a description by a single multidimensional dynamic field. Figure 21 illustrates the idea (based on simulations explained below). In the simplest case, two choices might be possible for either of two parameters—say, direction, *x,* and amplitude, *y.* This makes for a total of four possible movement parameter vectors. When prior information is given about amplitude, the two-dimensional field is preactivated at the two locations corresponding to the two directions at the precued amplitude. Specific input operates from this preactivated state, reducing buildup time compared with the case in which no preactivation is present. When prior information about direction is given, the field is preactivated in a region representing the two amplitudes at the precued direction. This preactivation merges into a single, monomodal preshape. Specific input now likewise operates from a preactivated level, shortening the distance to threshold. The sharing of preactivation across the two dimensions thus accounts for prior information about either parameter providing a reaction time advantage.

By contrast, if precuing direction was effective in reducing reaction time while precuing amplitude was not, then we would say that amplitude information cannot be processed before direction information has been provided. This would justify introducing two separate fields that are arranged in series.[4]

Identity of Parameters and Symmetry

The fact that precued information about different movement parameters reduces reaction time by different amounts was originally part of an argument that the description of a prepared movement can be broken up into different movement parameters (Rosenbaum, 1980). In the dynamic field, these different parameters are merely different coordinate axes. What is special about the axis representing direction compared with the axis representing amplitude? Might not just any system of coordinates be used to describe the field? Why, for instance, is the coordinate frame spanned by movement direction and movement amplitude preferred over the Cartesian coordinate frame spanned by the horizontal and the vertical movement extent (the coordinate frame typically used to characterize saccadic eye movements)? The answer is that although any coordinate system can be used, particular symmetries of the field may be best captured by a specific coordinate frame. In the dynamic field framework, questions about the different movement parameters become questions about symmetry properties of the field dynamics.

There are two places in the field dynamics that can be examined for symmetries: input and interaction. Symmetries of the input functions do not really inform us about symmetries of the movement parameter representation per se. They inform us about properties of the corresponding input channel. For instance, the visual specification of movement direction by a point of light at the

[4] Separate fields that are mutually coupled could also provide an account for the outcome of the precuing experiments. We do not further consider this option because it is not really functionally different from a single, two-dimensional field.

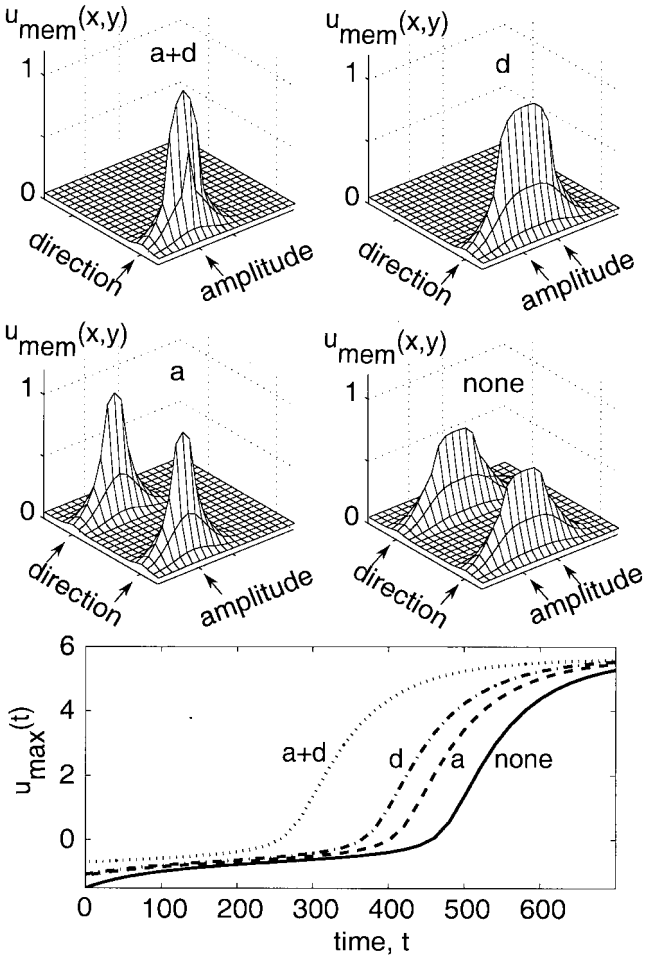

Figure 21. A two-dimensional field, $u(x, y)$, is used to account for differences between the processes of specification of the movement parameters direction, x, and amplitude, y, observed in the precuing paradigm of Rosenbaum (1980). Two choices are possible for each of the two dimensions. Arrows at the two parameter axes indicate the parameter values that the response signal may specify. The top four panels show stable states of the memory field, $u_{mem}(x, y)$, acting as task input into the movement parameter field under four different conditions of prior information: top left, both direction and amplitude (a + d) precued; top right, direction (d) precued; bottom left, amplitude (a) precued; bottom right, no parameter (none) precued. The task metrics lead to bimodal preshape along direction and monomodal preshape along amplitude. In the bottom frame, the temporal evolution of activation (in milliseconds) is compared across these four conditions. Activation is shown at the field location selected by specific input. Activation rises earliest when both parameters were precued (a + d), later when only direction was precued (d), later still when only amplitude was precued (a), and latest when no parameter was precued (none).

movement target might be symmetrical in the sense that the input strength does not depend on the direction in space in which the target lies. Imagine a somewhat artificial code in which the intensity of a sound specifies movement direction, to the right for higher intensity, to the left for lower intensity. In this case the input information might be asymmetrical—the loud sound may generate stronger input than the hushed sound. Measuring the dependence of reaction time in a simple response paradigm for different values of the specified parameter is a straightforward way to explore this asymmetry. For the remainder of this section we assume that the strength of the specific and task inputs are independent of the value specified by those inputs.

Symmetries of the interaction are, by contrast, properties of the dynamic field itself. We consider two types of symmetries, homogeneity and separability: 1. The interaction is *homogeneous* if its strength depends only on the distance between two parameter values, not on the values themselves.[5] Along the dimension of movement direction this means, for instance, that the inhibitory interaction between field sites 0° and 90° has the same strength as the inhibitory interaction between 10° and 100°, or between 20° and 110°, and so forth. Homogeneity of the interaction thus expresses a translation symmetry (invariance under translation in the space of movement parameters).

2. The interaction is *separable* if the way it depends on one dimension is independent of the way it depends on the other dimensions.[6] This implies that the evolution of the dynamical field along the different dimensions is independent. Thus, the concept of separability captures what is intuitively described as "independent processing of the different parameters" (e.g., Favilla et al., 1989; Rosenbaum, 1980). The mathematical definition involves products of functions that depend each on one dimension only (see Appendix A). In two dimensions, this definition may be visualized as follows: At some fixed location in the field, look for all places that interact at the same strength with that location. The set of such locations forms an ellipse, the main axes of which are aligned with the parameter axes. Varying the interaction strength varies the size of the ellipse, but its orientation is always aligned with the parameter axes. Thus, if the interaction is separable in a particular coordinate system, then the movement parameters represented along those axes can be said to be distinct and identifiable.

How may we find out if the interaction in a two-dimensional dynamic field is homogeneous and separable? The Rosenbaum (1980) paradigm again provides an experimental signature. Consider the two parameters amplitude and direction, with two levels for each parameter. If the smaller amplitude is precued, then two peaks of preactivation are positioned at the smaller amplitude and the two possible directions (see Figure 21). If the larger amplitude

[5] There are multiple definitions of the term *homogeneous* in different branches of mathematics. The definition used here is borrowed from the domain of convolution integrals (see, e.g., Arfken, 1985).

[6] This definition comes from the notion of separable integral kernels in mathematical physics. A two-variable kernel is separable if it can be written as a product of two functions, each depending only on one variable. A related use of this mathematical concept exists in psychophysics, where it is applied to receptive fields (Wandell, 1995, p. 143). Ashby and Townsend (1986) introduced the notions of perceptual, decisional, and temporal separability with goals very similar to ours. The global operational definitions of *perceptual separability* and *decisional separability* are close to ours. *Perceptual independence* is closest, at a formal level, to our mathematical definition of *separability*. The basic setting is very different from ours, however, with Ashby and Townsend operating on probability densities whereas we are operating on interaction kernels of a dynamic field.

is precued, then the two peaks are positioned at the larger amplitude. In a homogeneous separable field, these peaks are the same size as the two peaks for smaller amplitude. Therefore, the reaction time advantage offered by knowing amplitude is the same irrespective of whether the small or the large amplitude was precued. In Rosenbaum's (1980) analysis, this independence was tested by examining the statistical interaction in an analysis of variance of reaction time in which one factor described which parameter had been precued and the other factor was the precued value of the other parameter (the actual design was more complex). The absence of statistical interactions in that analysis supports the assumption that the dynamic field representing direction and amplitude (as well as effector) is homogeneous and separable. Converging evidence for homogeneity and separability of the representation of amplitude and direction comes from Bock and Arnold's (1992) observation that reaction time remained unchanged when the set of possible movements was varied such that the angular range of movement directions and the range of movement amplitudes remained constant.

Further support comes from the timed movement initiation paradigm. One set of experiments (Favilla et al., 1989; Hening, Favilla, & Ghez, 1988) involved isometric force pulses characterized by direction (up or down) and amplitude. When direction was fixed and only amplitude remained to be specified (Hening, Favilla, & Ghez, 1988), the time course of specification of amplitude was somewhat faster than when direction had to be specified as well (Favilla et al., 1989). This supports the notion that these two parameters are represented by a single two-dimensional dynamic field.[7]

The independence of amplitude and direction specification was probed in Favilla, Gordon, Hening, and Ghez (1990) by assigning different probabilities to the two levels of amplitude and of direction. The temporal evolution of the joint distribution of these parameters was sampled at a fixed but early time using the timed movement initiation protocol. The distribution of performed movement directions did not depend on which movement amplitude was performed and vice versa. In Ghez et al. (1997), two amplitudes and two directions occurred with equal probability, but the metrics of these choices were varied. In all cases it was found that the distribution of performed movement directions observed in different time slices did not depend on the metrics of the performed amplitudes and vice versa.

How Do Amplitude and Direction Differ?

What remains to be explained about the original Rosenbaum (1980) experiments is why knowing direction provides a stronger reduction in reaction time than knowing amplitude. We argue that the difference derives only from the fact that along the dimension of direction the two choices were at a larger metrical distance from each other than along the dimension of amplitude, leading to qualitatively different shapes of the patterns of preactivation (see Figure 21).

In the precuing paradigm, two sources of preshaping must be taken into account. First, the task setting involves only a small set of particular movements. The amplitudes and directions describing these movements are therefore preactivated in the dynamic field. The proposed mechanism for a dynamic memory field automatically generates such preactivation. Second, the precue itself generates input to the field. This input arises only once the precue signal is given. At that point, the pattern of preactivation in the dynamic field is modified consistent with the precued information: Preactivation is enhanced at the sites specified by the precue and is suppressed at the other sites.

In Rosenbaum's (1980) experiments the two possible movement directions were upward and downward, separated by the maximal distance of 180°. On the basis of the observations of Ghez et al. (1997), we expect a bimodal preshape along the dimension of direction. By contrast, the two amplitudes used in these studies differed by a factor of two, which leads to a monomodal preshape along the dimension of amplitude. The basic task input consists therefore of two peaks of activation positioned at the two movement directions, both centered on an average amplitude value (see the fourth panel in Figure 21). When direction is precued, the bimodal preshape is changed into a monomodal preshape, centered now only on the precued movement direction (see the top right panel in Figure 21). This speeds the subsequent specification processes significantly because the purely inhibitory input from the second preshape peak is removed. By contrast, when amplitude is precued, the preshape remains bimodal, although both peaks are shifted to the precued amplitude (see the third panel in Figure 21). Although this facilitates the subsequent specification processes, the associated growth of activation is still slowed by inhibition from the second preshape peak.

Thus, the difference between direction and amplitude in the precuing paradigm is due to the difference in the metric of the task along these two dimensions. By implication, the roles of direction and amplitude could be reversed if the metrics of the task were appropriately changed. For instance, the two amplitudes could be made to differ so strongly that bimodal preshape arises. At an amplitude ratio of 1:12, Ghez et al. (1997) recently reported bimodal histograms of amplitude for very early responses. Conversely, by choosing two directions that are less than about 60° apart, a monomodal preshape along the direction dimension could be created. We predict that this task metric will lead to a reversal of the roles of the two parameters, with amplitude precues now providing stronger reduction in reaction time than direction precues.

This account for Rosenbaum's (1980) results also provides insight into why the difference between the two parameters is reduced when stimulus–response compatibility is increased (see the last experiment in Rosenbaum, 1980; see also Anson, Hyland, Kötter, & Wickens, 2000; Goodman & Kelso, 1980). More highly compatible stimuli lead to stronger specific input, which reduces the relative importance of preshape. Because the difference between direction and amplitude is due to preshape, this difference is thus predicted to decrease for increasing stimulus–response compatibility.

Discussion

Three main ideas form the foundations of the dynamic field theory of movement preparation. First, movement parameters are

[7] Strictly speaking, an additional experimental condition is needed in which amplitude is kept fixed and direction remains to be specified. Knowing amplitude should also advance the specification of direction.

conceived of as dimensions of a field of activation, which inherits the metrics of the movement parameters. Localized patterns of activation represent information about motor plans, coded through the location of such patterns. Second, the process of specification of an upcoming movement is continuous in time. Its evolution is governed by a dynamical system of the activation field, which integrates different inputs. Interactions within the field lead to the self-stabilization of localized patterns of activation that represent motor plans. Third, the field dynamics receives input not only from channels of sensory information specific to the upcoming movement but also from a representation of the task environment. This representation may arise from various sources, such as from precued information, from the perceptual layout of the task environment, or from the recent motor history, which is accumulated in a second activation field with slower dynamics. The input from this representation preshapes the movement parameter field, preactivating parameter values relevant to the task.

A mathematical model of movement preparation was formulated based on these ideas. The model provided an account for a large number of experimental facts, including the influence of the number, probability, and metrics of the choices on the time course of movement preparation. The classical stimulus uncertainty effect was obtained as a limit case of the model. The balance between the two sources of input provided an account for stimulus–response compatibility that explained why number and probability of choice affect movement preparation less in more compatible tasks.

Simulations that accounted for these various effects were generated by establishing relationships between values of the model parameters and particular experimental signatures (see Appendix C). This means that many of the assumptions in the model are tested by published experiments. Beyond specific predictions, the consistent description of a set of experimental results based on tested assumptions is, therefore, a strong result.

Metrics

The metrics of represented movement parameters are foundational for the dynamic field account in two respects. First, movement preparation takes place over a continuous metrical space. This leaves signatures in the metrics of performed movements. Direct evidence for the continuity in parameter space of movement preparation comes from the experiments in the timed movement initiation paradigm (Ghez et al., 1990, 1997), in which intermediate values of cued movement parameters are produced early during movement preparation. Second, through preshaping by task input the metrics of the task environment matter. Direct evidence for effects of task metrics comes from experiments demonstrating the dependence of reaction time on the metrical distance between alternatives (Fiori et al., 1974). The dependence of movement preparation on the metrics of the movement task has been largely ignored in theoretical and experimental work. We have shown that effects of task metrics interact with the classical effects of probability of choice. This demonstrates dramatically that not only the amount of information to be processed but also its contents matter.

The metrics of representations are also conceptually important in the realms of perception and cognition. In the recognition of three-dimensional objects or faces, for instance, an appropriately defined metrical distance between learned and test stimuli affects reaction time (Bülthoff & Edelman, 1992; Shepard & Metzler, 1971). More generally, the metrics of similarity have been identified as an important factor in categorization (Nosofsky, 1992; Shepard, 1964). Note, however, that the effect of stimulus metrics on discrimination is the opposite of the effect of task metrics on movement preparation: When two stimuli are at a closer metrical distance, response time in a discrimination paradigm increases (Johnson, 1939), whereas when two movements are at a closer metrical distance, response time in a movement preparation paradigm decreases (Fiori et al., 1974).

The emphasis on metrics leads to new questions and new approaches to analysis: What is the internal structure, the symmetry, the homogeneity of movement representations? Over which distances in parameter space is information spread and fused? How do the metrics of movement representations evolve with learning and development? When more than one movement parameter is considered, these questions are interrelated with questions about the information-processing architecture of movement preparation. Rosenbaum (1980) illustrated the subtlety of this interrelation. His discovery of intrinsic differences between different movement parameters such as extent, direction, or limb was used to make inferences about a hierarchical information-processing architecture of the movement preparation system. Our account for these same differences ascribed them to the particular metrical structure of the task environment used in these experiments. The common ground, however, is the symmetries of the system, which may provide a basis for integrating dynamic ideas with ideas about information-processing architectures (e.g., Ashby & Townsend, 1986; Garner, 1974; Townsend & Ashby, 1983).

Dynamics

Patterns of activation of the dynamic field evolve continuously in time. This second foundational assumption is most directly supported by the experimental results obtained in the timed movement initiation paradigm (Ghez et al., 1990). The conventional reaction time paradigm offers a glimpse of temporal continuity when range effects are observed for early but not for late responses (Hening, Vicario, & Ghez, 1988; Poulton, 1981).

More specifically, the dynamic field approach postulates that the representation of movement parameters evolves as a dynamical system. The analogous assumption for perceptual representations underlies Grossberg's (1973, 1980, 1988) classical work. In decision theory, a closely related framework has been put forward by Busemeyer and Townsend (1993). Like the former, but unlike the latter, our dynamics is strongly nonlinear, fundamentally for the same reason as in Grossberg's work: to enable the representation itself to generate decisions in the face of ambiguous information (see Figure 3). By contrast, in decision field theory, probability distributions evolve as described by a (linear) dynamical system. Decisions are generated from events, involving criteria set from the outside, somewhat like in diffusion models of response generation (Link, 1992; Luce, 1986; Ratcliff, 1978).

Our primary motivation for postulating dynamical systems as the basis for understanding the continuous evolution of movement representations has been, however, the concept of dynamic stability (Schöner & Kelso, 1988b). Although generating a self-stabilized peak of activation requires passage through an instability (see Figure 2), once such a peak has been established, it is stably linked to on-line sensory information. Stability thus provides the

basis for an integrated account of movement representation and motor control. The instability traversed momentarily when a peak is first generated is a discrete event that emerges from the underlying temporally continuous system. This observation is interesting in relation to older debates about the temporal continuity or discreteness of processes underlying the specification of movement (for reviews, see McClelland, 1979; Miller, 1988; Sternberg, 1969).

Task

Fundamentally, most classical reaction time effects are reflections of the task environment in which any single motor act takes place. How else would, for instance, the number of choices affect the preparation process? Somehow, the fact that these other choices exist must prestructure the motor system. That prestructuring may take place in various ways, including conscious understanding of the task (when, for instance, a participant is instructed about the possible choices), learning that results from prior motor experience (when, for instance, the probability of targets is experienced over a block of trials), and perception (when, for instance, a number of locations are perceptually marked as potential movement targets).

The dynamic field theory accounts directly for the role of the task environment in movement preparation. The movement parameter field is preshaped by excitatory input that reflects the task environment. That input may result from one of the many sources through which task environments may be sensed. The most interesting source of specification of the task environment is, perhaps, the prior motor history of the system. This has been explicitly modeled through a dynamic preshape field, in which a memory trace of the dynamic field representing movement parameters is maintained.

In a more abstract sense, the dynamic field autonomously generates instances of the dimensions it represents in the form of self-stabilized peaks of activation. These instances are characterized by their location within the field and, thus, by the value of the movement parameter that they represent. For instance, in a task involving a certain number of choices, the field is preshaped at the corresponding locations of the movement parameter field, and a self-sustained peak is generated at a cued location. Thus, the basic units that represent choices emerge from the field dynamics.

By contrast, information-processing models of response preparation, although specific to the task, typically do not address how the structure of the task comes to be part of the system and how the system adjusts to changed task environments. For instance, a number of units or activation variables are assumed beforehand to designate particular choices (e.g., Grice et al., 1982).

Connectionist learning models (e.g., Rumelhart, McClelland, & Group, 1986) are closer in spirit to the theoretical framework proposed here. Through their learning rules, they incorporate part of the task environment into the system. In fact, the preshape dynamics could be alternatively formulated through a learning dynamics that modifies the input strength at preshaped locations in the field. Connectionist models have not typically used strong nonlinearity in the sense we defined it, and making learning rules work together with instabilities and self-stabilized peaks remains a technical challenge requiring further work.

What might be the functional significance of preshaping? On the basis of the experimental manifestations of preshape, one might be tempted to think of preshape as a mechanism that makes the system react faster in familiar environments. In more natural settings this seems a somewhat secondary factor, however. Similarly, the ability to generate a good "default" answer under conditions of reduced or incomplete information does not appear to be particularly powerful in more ecological conditions. A more abstract interpretation of preshape recognizes that only activated parts of representations contribute to interaction. Interaction is the basis for the generation of unique integrated responses in the face of variable and complex sensory information. Preactivating those parts of the motor representation about which expectations exist increases the potential for these expectations to contribute to the integration and decision processes.

Preshape reduces the dependence of the system on sensory input. Sensory information impinges on a system that is never a tabula rasa. In fact, it is important to realize that a nonprestructured system is never observable. Any experimental paradigm, even if aimed at the study of input channels and the forward flow of information, induces preactivation through the limited and structured sensorimotor repertoire it generates. Experiments must be interpreted in light of this insight.

Finally, the pervasive dependence of movement preparation on the task environment raises epistemological questions. In which sense is a theory of movement preparation possible? Is it necessary that such a theory provide an exhaustive account for all possible task environments? Our attitude has been to develop a theoretical language in which relevant constraints can be expressed. That language provides a method of analysis. For instance, the different results probing the contribution of preshape and those probing the contribution of specific input can be used to study such inputs experimentally. A theoretical account of movement preparation is ultimately achieved if lawful aspects of how changes in sensory, motor, or task environments lead to changes in the processes of movement preparation are discovered and described.

Neurophysiology

We have used neural jargon, such as *activation, input, threshold,* and so forth. What is the relationship between the dynamic field theory and neurophysiology? In a nutshell, although the concepts of the dynamic field theory are abstract, they are neurophysiologically plausible and lend themselves to extensions of the theory into the neural domain.

The dynamic field is defined over task space (spanned by movement parameters), not over some anatomically defined space. Nevertheless, the field can be linked to patterns of neural activation in two different ways. In the first case, a topographical mapping between a stimulus or task parameter and the anatomical location of neurons makes it possible to directly interpret the distribution of activation on the anatomical substrate as a dynamic field. The superior colliculus provides an excellent example. Both its sensory and its motor layer map topographically the endpoints of visually induced saccades (Robinson, 1972; for a review, see Sparks, 1986). Each neuron has a fairly large unimodal receptive field of saccadic end positions. Neurons that are close to each other on the surface of the superior colliculus have similar receptive fields. During any single visually driven saccade, a large part of

the superior colliculus is activated. By reversibly deactivating small patches of the superior colliculus, Sparks and his collaborators (for a review, see Sparks & Groh, 1995) have demonstrated that all of this widely distributed activation contributes to the specification of the saccadic endpoint.

The distribution of activation on the collicular surface could thus be usefully interpreted as a neural realization of a dynamic field representing the movement parameter saccadic endpoint. A localized pattern of activation represents a well-defined saccade. Kopecz and Schöner (1995) formulated a dynamic field model of the specification of saccadic eye movements along such lines and critically discussed its relation to collicular neurophysiology.

In the absence of topography, this direct mapping of neural patterns of activation onto patterns of activation in dynamic fields is not possible. Topography is violated in relevant domains. The tuning curves of neurons in primary and premotor cortex to global movement parameters such as movement direction (Georgopoulos, Kalaska, Caminiti, & Massey, 1982) or movement amplitude (Fu, Suarez, & Ebner, 1993), for instance, reveal no apparent topographic order. Neighboring neurons may have quite different "preferred directions," for example. Even in the sensory domain, the microstructure of cortical maps shows significant deviations from topography, which limit the power of this direct approach.

The second, alternative avenue is to use the ideas of a population representation of movement parameters pioneered by Georgopoulos and colleagues (for a recent review, see Georgopoulos, 1995). The starting point is to view the population representation as a transformation from a representation in anatomical coordinates (where neurons are characterized by their location on the cortical surface) to a representation in functional coordinates (where neurons are characterized by the value of the task parameter they respond to most strongly). Extending the concept of a population vector (Georgopoulos, Schwartz, & Kettner, 1986), one can compute the distribution of activation in the space of movement directions as an estimate of an underlying dynamic field representing movement direction (Erlhagen, Bastian, Jancke, Riehle, & Schöner, 1999). Bastian, Riehle, Erlhagen, and Schöner (1998) performed such a estimation based on the tuning curves to movement direction of neurons in motor and premotor cortex. They varied experimentally the range of movement directions within which monkeys expected an upcoming movement command. The distribution of population activation over the parameter movement direction was shown to reflect this range. In the period between a precue that indicated the different movement directions possible on a particular trial and the response signal that specified which movement direction had to be realized on that trial, the distribution of population activation was broader when a wider range of directions was precued than when a narrower range was precued. The distribution of population activation thus displayed preshaping in response to the precue!

The concept of self-generation and stabilization of activation through cooperative interactions within a dynamic field has an obvious neural counterpart. There is ample anatomical support for cooperative interactions, in particular, through abundant intracortical connectivity (Braitenberg & Schüz, 1991), including recurrent loops that occur across areas. In motor cortex, connectivity among neurons was found to depend in a graded fashion on the difference between the preferred parameter values represented by the neurons (Georgopoulos, Taira, & Lukashin, 1993), although this result is still subject to some technical discussions (see Fetz & Shupe, 1994; Georgopoulos, Taira, & Lukashin, 1994). Connectivity in visual areas has been shown to reflect the tuning of neurons in a manner compatible with the assumptions of dynamic field theory, in that similarly tuned neurons are more strongly connected (e.g., Ts'o, Gilbert, & Wiesel, 1986).

The original mathematical modeling on which the dynamic field equations are based (Amari, 1977; Wilson & Cowan, 1973) was motivated by cortical anatomy. More generally, neurally inspired models bear some similarity to concepts of the dynamic field approach. In particular, Grossberg and his students have used a very similar mathematical framework to ours to model the temporal evolution of neural activation (Bullock & Grossberg, 1988; Grossberg, 1973, 1980, 1988). Most neurally inspired modeling in the motor domain, however, is aimed at motor control, including trajectory formation and the problems of learning forward and inverse models, of adapting sensorimotor maps (for a recent review, see, e.g., Jordan, 1995), and of generating invariances through appropriate coordinate transforms (Bullock, Grossberg, & Guenther, 1993). By contrast, the preparation of movement and the integration of multiple sources of information that takes place at that level have not typically been addressed. Two recent exceptions are the work of Houk and colleagues, who have looked at self-generation mechanisms in models of the initiation of motor commands in cortical and subcortical structures (for a review, see Houk, Keifer, & Barto, 1995), and a model described, but not mathematically formalized by, Wickens, Hyland, and Anson (1994). Wickens and colleagues suggested that intracortical connections may favor particular patterns of activation. Adjusting these connectivities in response to the recent history of activation would thus lead to something like a preshaping mechanism.

The strong role played by the task and the task environment in the dynamic field perspective poses an interesting challenge to the interpretation of some neurophysiological data. For methodological reasons, unit recording typically is based on many trials, over which averages are computed. These trials come from highly trained animals that perform a narrowly defined task. Thus, in our terms, their motor representations are highly preshaped. What one is actually assessing, therefore, is the function of highly preshaped neural representations, not necessarily the general function of the neural substrate.

Limitations and Outlook

The dynamic field notion emphasizes the continuous ranges of values of movement parameters. However, some movement parameters seem to have discrete values. Selecting either the right or the left arm, for example, appears to be a discrete choice (although in natural settings both limbs may be activated to a degree). Although a dynamic model with interaction can be formulated for discrete activation variables, the field character and, thus, the metrics of the representation are lost.

A second issue is a larger one, which we can only hint at. At the outset we emphasized that the fact that movement plans can be updated anytime during the process of movement preparation as well as during the movement poses theoretical challenges, which the dynamic field approach is meant to address. The dynamic field provides an account of specification of movement parameters that is based on continuous time and that endows the representation of

these parameters with stability, both of which are prerequisites for dealing with continuous updating. We have provided, however, only the most rudimentary interface between the movement plan and the actual initiation and control of the movement in the form of the two read-out procedures we analyzed in the context of the timed movement initiation paradigm and the reaction time paradigm.

It is obvious that much more must be done to provide a complete account of how movement planning and motor control are integrated. This includes resolving issues such as what happens to the activation in the dynamic field after the movement act has been performed, how movement is timed and coordinated given a movement plan, how perturbations encountered during the movement may or may not affect the movement plan, how fixation demands in the initial or the final position affect the time course of movement initiation. First steps toward addressing such issues were made in the context of specifying visually induced saccadic eye movements in work we did with Klaus Kopecz (Kopecz, 1995; Kopecz & Schöner, 1995; Schöner, Kopecz, & Erlhagen, 1997). Limb movement provides more difficult challenges because both the control and the timing and coordination of limb movements are more flexible and complex. Because we have used the same theoretical setting to design and build working robot vehicles, we are confident that the loop with motor control, effector as well as sensory systems, can ultimately be closed (Bicho, Mallet, & Schöner, 2000; Schöner, Dose, & Engels, 1995).

We have concentrated on the process of preparing a movement as the exemplary problem around which the dynamic field concept and the idea of preshaping are formulated and tested. We are beginning to see, however, that these concepts can be applied within cognition beyond this particular problem, whenever metrics play an important role. We have begun, for instance, to look at spatial memory in this way (Spencer & Schöner, 1998) and have used the present framework to formulate a model of the Piagetian A-not-B effect (Thelen, Schöner, Scheier, & Smith, 2000). A goal of such extension of the dynamic field framework into forms of cognition that are further removed from the motor and sensory surfaces can be to keep the constraints of neurophysiology, of the physical body, and of the environment in the theoretical picture.

References

Amari, S. (1977). Dynamics of pattern formation in lateral-inhibition type neural fields. *Biological Cybernetics, 27,* 77–87.

Amari, S., & Arbib, M. A. (1977). Competition and cooperation in neural nets. In J. Metzler (Ed.), *Systems neuroscience* (pp. 119–165). New York: Academic Press.

Anson, J. G., Hyland, B. I., Kötter, R., & Wickens, J. R. (2000). Parameter precuing and motor preparation. *Motor Control, 4,* 221–231.

Arfken, G. (1985). *Mathematical methods for physicists* (3rd ed.). San Diego, CA: Academic Press.

Arnold, V. I. (1973). *Ordinary differential equations.* Cambridge, MA: MIT Press.

Ashby, F. G., & Townsend, J. T. (1986). Varieties of perceptual independence. *Psychological Review, 93,* 154–179.

Bastian, A., Riehle, A., Erlhagen, W., & Schöner, G. (1998). Prior information preshapes the population representation of movement direction in motor cortex. *NeuroReport, 9,* 315–319.

Bicho, E., Mallet, P., & Schöner, G. (2000). Target representation on an autonomous vehicle with low-level sensors. *The International Journal of Robotics Research, 19,* 424–447.

Bock, O., & Arnold, K. (1992). Motor control prior to movement onset: Preparatory mechanisms for pointing at visual targets. *Experimental Brain Research, 90,* 209–216.

Braitenberg, V., & Schüz, A. (1991). *Anatomy of the cortex.* Berlin, Germany: Springer-Verlag.

Bullock, D., & Grossberg, S. (1988). Neural dynamics of planned arm movements: Emergent invariants and speed–accuracy properties during trajectory formation. *Psychological Review, 95,* 49–90.

Bullock, D., Grossberg, S., & Guenther, F. (1993). A self-organizing neural model of motor equivalence reaching and tool use by a multijoint arm. *Journal of Cognitive Neuroscience, 5,* 408–435.

Bülthoff, H. H., & Edelman, S. (1992). Psychophysical support for a two-dimensional view interpolation theory of object recognition. *Proceedings of the National Academy of Sciences (USA), 89,* 60–64.

Busemeyer, J. R., & Townsend, J. T. (1993). Decision field theory: A dynamic–cognitive approach to decision making in an uncertain environment. *Psychological Review, 100,* 432–459.

Craft, J. L., & Simon, J. R. (1970). Processing symbolic information from a visual display: Interference from an irrelevant directional cue. *Journal of Experimental Psychology, 83,* 415–420.

Erlhagen, W. (1997). *Lokalisierte, stationäre Verteilungen in neuronalen Feldern* [Localized, stationary distributions in neural fields]. Unpublished doctoral dissertation, Department of Mathematics, Ruhr-Universität Bochum, Bochum, Germany.

Erlhagen, W., Bastian, A., Jancke, D., Riehle, A., & Schöner, G. (1999). The distribution of neuronal population activation (DPA) as a tool to study interaction and integration in cortical representations. *Journal of Neuroscience Methods, 94,* 53–66.

Favilla, M. (1997). Reaching movements: Concurrency of continuous and discrete programming. *NeuroReport, 8,* 3973–3977.

Favilla, M., Gordon, J., Ghilardi, M. F., & Ghez, C. (1990). Discrete and continuous processes in the programming of extent and direction in multijoint arm movements. *Society for Neuroscience Abstracts, 16,* 1089.

Favilla, M., Gordon, J., Hening, W., & Ghez, C. (1990). Trajectory control in targeted force impulses: VII. Independent setting of amplitude and direction in response preparation. *Experimental Brain Research, 79,* 530–538.

Favilla, M., Hening, W., & Ghez, C. (1989). Trajectory control in targeted force impulses: VI. Indendent specification of response amplitude and direction. *Experimental Brain Research, 75,* 280–294.

Fetz, E. E., & Shupe, L. E. (1994, March 4). Measuring synaptic interactions. *Science, 263,* 1295–1296.

Fiori, N., Semjen, A., & Requin, J. (1974). Analyse chronométrique du pattern préparatoire à un mouvement spatialment orienté. Résultats préliminaires [Chronometric analysis of the preparatory processes of spatially directed movements. Preliminary results]. *Le Travail Humain, 37,* 229–248.

Fitts, P. M., & Posner, M. I. (1967). *Human performance.* Belmont, CA: Brooks/Cole.

Fu, Q.-G., Suarez, J. I., & Ebner, T. J. (1993). Neuronal specification of direction and distance during reaching movements in the superior precentral premotor area and primary motor cortex of monkeys. *Journal of Neurophysiology, 70,* 2097–2116.

Garner, W. R. (1974). *The processing of information and structure.* Hillsdale, NJ: Erlbaum.

Georgopoulos, A. P. (1986). On reaching. *Annual Reviews of Neuroscience, 9,* 147–170.

Georgopoulos, A. P. (1991). Higher order motor control. *Annual Reviews of Neuroscience, 14,* 361–377.

Georgopoulos, A. P. (1995). Motor cortex and cognitive processing. In M. S. Gazzaniga (Ed.), *The cognitive neurosciences* (pp. 507–517). Cambridge, MA: MIT Press.

Georgopoulos, A. P., Kalaska, J. F., Caminiti, R., & Massey, J. T. (1982).

On the relations between the direction of two-dimensional arm movements and cell discharge in primate motor cortex. *Journal of Neuroscience, 2,* 1527–1537.

Georgopoulos, A. P., Schwartz, A. B., & Kettner, R. E. (1986, September 26). Neural population coding of movement direction. *Science, 233,* 1416–1419.

Georgopoulos, A. P., Taira, M., & Lukashin, A. (1993, April 2). Cognitive neurophysiology of the motor cortex. *Science, 260,* 47–52.

Georgopoulos, A. P., Taira, M., & Lukashin, A. V. (1994, March 4). Measuring synaptic interactions: Response. *Science, 263,* 1296–1297.

Ghez, C., Favilla, M., Ghilardi, M. F., Gordon, J., Bermejo, R., & Pullman, S. (1997). Discrete and continuous planning of hand movements and isometric force trajectories. *Experimental Brain Research, 115,* 217–233.

Ghez, C., Hening, W., & Favilla, M. (1990). Parallel interacting channels in the initiation and specification of motor response features. In M. Jeannerod (Ed.), *Attention and performance* (Vol. 13, pp. 265–293). Hillsdale, NJ: Erlbaum.

Ghez, C., Hening, W., & Gordon, J. (1991). Organization of voluntary movement. *Current Biology, 1,* 664–671.

Goodale, M. A., Pélisson, D., & Prablanc, C. (1986). Large adjustments in visually guided reaching do not depend on vision of the hand or perception of target displacement. *Nature, 320,* 748–750.

Goodman, D., & Kelso, J. A. S. (1980). Are movements prepared in parts? Not under compatible (naturalized) conditions. *Journal of Experimental Psychology: General, 109,* 475–495.

Grice, G. R., Nullmeyer, R., & Spiker, V. A. (1982). Human reaction time: Toward a general theory. *Journal of Experimental Psychology: General, 111,* 135–153.

Grossberg, S. (1973). Contour enhancement, short term memory, and constancies in reverberating neural networks. *Studies in Applied Mathematics, 52,* 217–257.

Grossberg, S. (1980). Biological competition: Decision rules, pattern formation, and oscillations. *Proceedings of the National Academy of Sciences (USA), 77,* 2338–2342.

Grossberg, S. (1988). Nonlinear neural networks: Principles, mechanisms, and architectures. *Neural Networks, 1,* 17–61.

Hening, W., Favilla, M., & Ghez, C. (1988). Trajectory control in targeted force impulses: V. Gradual specification of response amplitude. *Experimental Brain Research, 71,* 116–128.

Hening, W., Vicario, D., & Ghez, C. (1988). Trajectory control in targeted force impulses: IV. Influences of choice, prior experience and urgency. *Experimental Brain Research, 71,* 103–115.

Hick, W. E. (1952). On the rate of gain of information. *Quarterly Journal of Experimental Psychology, 4,* 11–26.

Hietanen, J. K., & Rämä, P. (1995). Facilitation and interference occur at different stages of processing in the Simon paradigm. *European Journal of Cognitive Psychology, 7,* 183–199.

Hinton, G. E. (1984). Parallel computations for controlling an arm. *Journal of Motor Behavior, 16,* 171–194.

Hirsch, M. W. (1989). Convergent activation dynamics in continuous time networks. *Neural Networks, 2,* 331–349.

Houk, J. C., Keifer, J., & Barto, A. G. (1995). Distributed motor commands in the limb premotor network. *Trends in Neurosciences, 16,* 27–33.

Hyman, R. (1953). Stimulus information as a determinant of reaction time. *Journal of Experimental Psychology, 45,* 188–196.

Johnson, D. M. (1939). Confidence and speed in the two-category judgment. *Archives of Psychology, 241,* 1–52.

Jordan, M. I. (1990). Motor learning and the degrees of freedom problem. In M. Jeannerod (Ed.), *Attention and performance* (Vol. 13, pp. 796–836). Hillsdale, NJ: Erlbaum.

Jordan, M. I. (1995). Computational motor control. In M. S. Gazzaniga (Ed.), *The cognitive neurosciences* (pp. 597–609). Cambridge, MA: MIT Press.

Keele, S. W. (1981). Behavioural analysis of movement. In V. B. Brooks (Ed.), *Handbook of physiology. Sect. 1: The nervous system. Vol. 2. Motor control* (Pt. 2, pp. 1391–1414). Bethesda, MD: American Physiological Society.

Keele, S. W. (1986). Motor control. In K. R. Boff, L. Kaufman, & J. P. Thomas (Eds.), *Handbook of perception and human performance* (pp. 30-1–30-60). New York: Wiley.

Kishimoto, K., & Amari, S. (1979). Existence and stability of local excitations in homogeneous neural fields. *Journal of Mathematical Biology, 7,* 303–318.

Konen, W., Maurer, T., & Malsburg, C. von der. (1994). A fast dynamic link matching algorithm for invariant pattern recognition. *Neural Networks, 7,* 1019–1030.

Kopecz, K. (1995). Saccadic reaction times in gap/overlap paradigms: A model based on integration of intentional and visual information on neural, dynamic fields. *Vision Research, 35,* 2911–2925.

Kopecz, K., & Schöner, G. (1995). Saccadic motor planning by integrating visual information and pre-information on neural, dynamic fields. *Biological Cybernetics, 73,* 49–60.

Kornblum, S., Hasbroucq, T., & Osman, A. (1990). Dimensional overlap: Cognitive basis for stimulus–response compatibility—A model and a taxonomy. *Psychological Review, 97,* 253–270.

Lee, D., & Young, D. S. (1986). Gearing action to the environment. In H. H. Hever & F. C. Fromm (Eds.), *Generation and modulation of action patterns* (pp. 217–230). Berlin, Germany: Springer-Verlag.

Link, S. (1992). *The wave theory of difference and similarity.* Hillsdale, NJ: Erlbaum.

Lu, C.-H., & Proctor, R. W. (1995). The influence of irrelevant location information on performance: A review of the Simon and spatial Stroop effect. *Psychonomic Bulletin & Review, 2,* 174–207.

Luce, R. D. (1986). *Response times.* Oxford, England: Oxford University Press.

McClelland, J. L. (1979). On the time relations of mental processes: A framework for analyzing processes in cascade. *Psychological Review, 86,* 287–330.

Mikhailov, A. (1990). *Foundations of synergetics: Vol. 1. Distributed active systems.* Berlin, Germany: Springer-Verlag.

Miller, J. O. (1988). Discrete and continuous models of human information processing: Theoretical distinctions and empirical results. *Acta Psychologica, 67,* 191–257.

Murray, J. D. (1989). *Mathematical biology.* Berlin, Germany: Springer-Verlag.

Nosofsky, R. M. (1992). Similarity scaling and cognitive process models. *Annual Review of Psychology, 43,* 25–53.

Poulton, E. C. (1981). Human manual control. In V. B. Brooks (Ed.), *Handbook of physiology. Sect. 1: The nervous system. Vol. 2. Motor control* (Pt. 2, pp. 1337–1389). Bethesda, MD: American Physiological Society.

Prablanc, C., & Martin, O. (1992). Autonomous control during hand reaching at undetected two-dimensional target displacements. *Journal of Neurophysiology, 67,* 455–469.

Ratcliff, R. (1978). A theory of memory retrieval. *Psychological Review, 85,* 59–108.

Riehle, A., MacKay, W. A., & Requin, J. (1994). Are extent and force independent movement parameters? Preparation- and movement-related neuronal activity. *Experimental Brain Research, 99,* 56–74.

Robinson, D. A. (1972). Eye movements evoked by collicular stimulation in the alert monkey. *Vision Research, 12,* 1795–1808.

Rosenbaum, D. A. (1980). Human movement initiation: Specification of aim, direction, and extent. *Journal of Experimental Psychology: General, 109,* 444–474.

Rosenbaum, D. A. (1991). *Human motor control.* San Diego, CA: Academic Press.

Rosenbaum, D. A., Loukopoulos, L. D., Meulenbroek, R. G. L., Vaughan,

J., & Engelbrecht, S. E. (1995). Planning reaches by evaluating stored postures. *Psychological Review, 102,* 28–67.
Rubichi, S., Nicoletti, R., Umiltà, C., & Zorzi, M. (2000). Response strategies and the Simon effect. *Psychological Research, 63,* 129–136.
Rumelhart, D. E., McClelland, J. L., & Group, T. P. R. (Eds.). (1986). *Parallel distributed processing: Vol. 1. Foundations.* Cambridge, MA: MIT Press.
Schöner, G., Dose, M., & Engels, C. (1995). Dynamics of behavior: Theory and applications for autonomous robot architectures. *Robotics and Autonomous Systems, 16,* 213–245.
Schöner, G., & Kelso, J. A. S. (1988a). A dynamic theory of behavioral change. *Journal of Theoretical Biology, 135,* 501–524.
Schöner, G., & Kelso, J. A. S. (1988b). Dynamic pattern generation in behavioral and neural systems. *Science, 239,* 1513–1520.
Schöner, G., Kopecz, K., & Erlhagen, W. (1997). The dynamic neural field theory of motor programming: Arm and eye movements. In P. G. Morasso & V. Sanguineti (Vol. Eds.) & G. E. Stelmach & P. A. Vroon (Series Eds.), *Advances in psychology: Self-organization, computational maps and motor control* (Vol. 119, pp. 271–310). Amsterdam: Elsevier-North Holland.
Schouten, J. F., & Bekker, J. A. M. (1967). Reaction time and accuracy. *Acta Psychologica, 27,* 143–153.
Shepard, R. N. (1964). Attention and the metrical structure of the similarity space. *Journal of Mathematical Psychology, 1,* 54–87.
Shepard, R. N., & Metzler, J. (1971, February 19). Mental rotation of three-dimensional objects. *Science, 171,* 901–903.
Sparks, D. L. (1986). Translation of sensory signals into commands for the control of saccadic eye movements: Role of the primate superior colliculus. *Physiological Review, 66,* 118–171.
Sparks, D. L., & Groh, J. M. (1995). The superior colliculus: A window for viewing issues in integrative neuroscience. In M. S. Gazzaniga (Ed.), *The cognitive neurosciences* (pp. 565–584). Cambridge, MA: MIT Press.
Spencer, J. P., & Schöner, G. (1998). A dynamic neural field theory of location memory. *Society for Neuroscience Abstracts, 24,* 65.1.
Sperling, G., & Sondhi, M. M. (1968). Model for visual luminance discrimination and flicker detection. *Journal of the Optical Society of America, 58,* 1133–1145.
Sternberg, S. (1969). The discovery of processing stages: Extensions of Donder's method. In W. G. Koster (Ed.), *Attention and performance* (Vol. 2, pp. 276–315). Amsterdam: North-Holland.
Thelen, E., Schöner, G., Scheier, C., & Smith, L. (2000). The dynamics of embodiment: A field theory of infant perseverative reaching. *Brain and Behavioral Sciences, 24,* 1–33.
Townsend, J. T., & Ashby, F. G. (1983). *Stochastic modelling of elementary psychological processes.* Cambridge, England: Cambridge University Press.
Ts'o, D., Gilbert, C. D., & Wiesel, T. (1986). Relationships between horizontal interactions and functional architecture in cat striate cortex as revealed by cross-correlation analysis. *Journal of Neuroscience, 6,* 1160–1170.
Vidal, F., Bonnet, M., & Macar, F. (1991). Programming response duration in a precueing reaction time paradigm. *Journal of Motor Behavior, 23,* 226–234.
Wandell, B. A. (1995). *Foundations of vision.* Sunderland, MA: Sinauer Associates.
Wickens, J., Hyland, B., & Anson, G. (1994). Cortical cell assemblies: A possible mechanism for motor programs. *Journal of Motor Behavior, 26,* 66–82.
Wilson, H. R., & Cowan, J. D. (1973). A mathematical theory of the functional dynamics of cortical and thalamic nervous tissue. *Kybernetik, 13,* 55–80.
Zorzi, M., & Umiltà, C. (1995). A computational model of the Simon effect. *Psychological Research, 58,* 193–205.

Appendix A

The Amari Neural Field Dynamics

Field Dynamics in One Dimension

How can the theoretical concept of a dynamic field be used to formulate mathematical models of movement preparation? The key assumption constraining such models is the existence and stability of stationary localized solutions of a field dynamics. Unfortunately, from a mathematical point of view, field dynamics are not easily classified or even analyzed with respect to this constraint. This is due, in large part, to the necessarily nonlinear nature of such solutions and the absence of strong constraints from boundary conditions (see Erlhagen, 1997, for a discussion). What is available is a collection of mathematical models, analysis of which has led to the identification of such solutions and their properties (e.g., Amari, 1977; Amari & Arbib, 1977; Kishimoto & Amari, 1979; Mikhailov, 1990; Murray, 1989).

Our strategy has been to work within the framework of a particular class of models, the "neural" fields first analyzed by Amari (1977) for localized solutions. The exact solutions available within this model make it possible to determine some parameter values based on analytic arguments. Moreover, the limit cases of strong and weak input relative to the within-field cooperative interaction can be mathematically treated, which helps both to clarify the concepts and to analyze effects.

The simplest version of the Amari (1977) neural field model for a one-dimensional scalar field $u(x, t)$, where x lies within an interval, reads

$$\tau \dot{u}(x, t) = -u(x, t) + h + S(x, t) + \int w(x - x') f[u(x', t)] dx'. \quad \text{(A1)}$$

The parameter τ determines the time scale of the dynamics. The parameter h fixes the overall level of activation, which is relevant in relation to the threshold function, f. The intrafield interaction takes the form of a convolution over the thresholded field $f(u)$ with homogeneous convolution kernel w. The threshold function can be a step function or a smoother sigmoidal form such as

$$f(u) = \frac{1}{1 + \exp[-\beta(u - u_0)]}, \quad \text{(A2)}$$

where β controls the steepness and u_0 the position of the inflection point of the nonlinear function (see Figure 4 for illustration). In either case only sufficiently activated parts of the field contribute to intrafield interaction. The convolution kernel typically has a form as illustrated in Figure 4b: Over small distances the intrafield interaction is excitatory, over medium distances inhibitory, and over larger distances either inhibitory (global inhibition) or zero. This form of interaction is widely applied in cortical modeling and often referred to as *lateral inhibition.* The kernel used in our modeling work is

$$w(x - x') = w_{\text{excite}} \exp\left[\frac{-(x - x')^2}{2\sigma_w^2}\right] - w_{\text{inhibit}}. \quad \text{(A3)}$$

The parameter σ_w determines the width of the excitatory part of the kernel. Other fields (such as specific and task input) couple additively into the field dynamics through $S(x, t) = S_{\text{task}}(x, t) + S_{\text{spec}}(x, t)$. Spatial continuity of the

resulting neural field distributions is warranted for spatially continuous input distributions by the integro-differential form of the dynamics.

In the limit case of weak or absent input, $S(x, t) \ll 1$, a complete discussion of the phase diagram of this model has been given by Amari (1977) for step-function threshold and by Kishimoto and Amari (1979) for smooth threshold functions. We briefly summarize these results as relevant for our purposes:

1. In the absence of input, the homogeneous solution $u(x) = h$ exists and is stable for sufficiently small parameter h.
2. Solutions with a single hump of activation exist and are stable for intermediate values of h. These solutions are stable in the sense that the field relaxes to the stationary state following perturbations of their form. However, in the absence of inhomogeneous input, $S(x)$, these solutions are neutrally stable with respect to their location in the field: They can be shifted arbitrarily within the field. The homogeneous and the localized solutions coexist bistably for small input.
3. Stronger localized input destabilizes the homogeneous solution. Such input induces a localized peak of activation. If input is removed and the system is in the bistable regime, the localized peak relaxes to the self-generated localized solution. In this way, input may set a localized peak, which is stabilized by interaction even in the absence of input.

To address the variability of the parameter specification process, we endow the field with stochastic properties by adding stochastic forces to the dynamics. On the basis of standard assumptions (noise originates from many independent sources of variability, noise is fast compared with dynamics, noise is never zero), the stochastic forces can be modeled by uncorrelated Gaussian processes, $q\zeta(x, t)$, which add into the field dynamics (Equation A1). The noise strength, q, is an additional parameter.

Field Dynamics in Two Dimensions

It is straightforward to generalize to multiple dimensions the basic concepts of the field dynamics and the mechanisms that ensure the existence of localized, stable distributions of activation. For simplicity, we give the equations in two dimensions only.

Consider a two-dimensional field spanned over the parameter dimensions x and y. We use the notation $u(x, y, t)$ to describe the level of activity at location (x, y) and time t. The dynamic equation has the same form as Equation A1:

$$\tau\dot{u}(x, y, t) = -u(x, y, t) + h + S(x, y, t) + \int\int w(x, x', y, y')f[u(x', y', t)]dx'dy'. \quad \text{(A4)}$$

As in the one-dimensional case, the strength of interaction, now represented by a two-dimensional interaction kernel $w(x, x', y, y')$, is assumed to depend only on the metrical distance between the interacting locations, taken separately along the x and the y dimensions:

$$w(x, x', y, y') = w(x - x', y - y'). \quad \text{(A5)}$$

This is the assumption of *homogeneity*.

For a step-function nonlinearity and an interaction kernel $w(x - x', y - y')$ consisting of local excitation and long range inhibition, it is possible to extend the methods of Amari (1977) to the two-dimensional case, deducing similar analytical results about the existence and stability of localized peak solutions (Konen, Maurer, & Malsburg, 1994).

In our simulations (see Figure 21), the kernel was chosen with constant, global inhibition, $w_{\text{inhibit},xy}$, and a two-dimensional Gaussian distribution for the excitatory part. Mathematically, the excitatory part was written as a product of two Gaussians that depend each only on one dimension, x or y (assumption of *separability*):

$$w(x - x', y - y') = w_{\text{excite},x} \exp\left[\frac{-(x - x')^2}{2\sigma_{w,x}^2}\right] w_{\text{excite},y} \exp\left[\frac{-(y - y')^2}{2\sigma_{w,y}^2}\right] - w_{\text{inhibit},xy}. \quad \text{(A6)}$$

Appendix B

Dynamics of the Memory Field

The dynamics of the memory field, $u_{\text{mem}}(x, t)$, models the adjustment of task input, $S_{\text{task}}(x)$, to changes in the task environment. In a probabilistic paradigm, for instance, changes of the probability of different choices lead to adjustment of response time and error within a few trials. The adjustment of the memory trace takes place, almost by definition, on a time scale larger than that characteristic of each individual trial, that is, larger than the time scale on which the movement parameter field itself evolves.

The dynamics of the memory field can be formulated within the framework of dynamic fields if two constraints are taken into account. First, multimodal and graded distributions of activation must exist as stable states. Such distributions represent the amount of preactivation of multiple target parameter values. Second, these stable states must adjust to ongoing changes in movement history or other sources of task input. In the absence of input to the memory field, however, activation must decay slowly. These constraints imply that we cannot operate within the bistable regime of the Amari (1977) equation, as that would lead to normalized self-sustained peaks. Moreover, the time scale at which the dynamics evolves must depend on the state of activation and on the presence of input. There are two different ways this can be achieved. Either a two-variable field is defined, in which each variable induces a separate time scale, or a nonlinear (multiplicative) relaxation mechanism can be used, in which the activation level itself modulates the time scale. As it is simpler, we adopted the second approach:

$$\tau_{\text{mem}}\dot{u}_{\text{mem}}(x, t) = -Au_{\text{mem}}(x, t) + u_{\text{mem}}(x, t)f[u_{\text{mem}}(x, t)] + I(x, t) - u_{\text{mem}}(x, t)\int w_{\text{mem}}(x - x')f[u_{\text{mem}}(x', t)]dx'. \quad \text{(B1)}$$

Here, A is a positive constant, $f(u_{\text{mem}})$ is the sigmoidal transfer function of Equation A2, $w_{\text{mem}}(x - x')$ is an interaction kernel, and $I(x, t)$ is the input that drives the memory field. We used a purely inhibitory and constant form of interaction, $w_{\text{mem}}(x - x') = w_{\text{mem,inhibit}}$, so that the interaction contribution is as follows:

$$-w_{\text{mem,inhibit}}\int f[u(x')]dx'. \quad \text{(B2)}$$

(*Appendixes continue*)

This sums all positive activation in the field and inhibits proportionally.

A spatially discrete version of Equation B1 is known as a *shunting inhibition cooperative network*, the computational properties of which have been extensively studied by several authors (reviewed by Grossberg, 1988; Hirsch, 1989). Those discretized dynamics are globally stable, so that the stable state is reached from any initial pattern of activation.

The first three terms of Equation B1 affect the time scale of relaxation of the field. For low levels of activation in the entire field, only the first term is relevant. This defines the time scale of the "empty" memory field, τ_{mem}/A, controlled by the parameter $A \ll 1$ such that the memory field is slower than the movement parameter field. The second and fourth term modify the time scale at site x if there is activation in the field. The second term, a local self-excitation, slows relaxation down. This term is responsible for keeping activation from decaying quickly in the absence of input. The fourth term, a global inhibition, increases the time scale if there is activation distributed in the field. This term drives adjustment of activation at site x in competition with activation at other sites x'. Finally, the third term represents input.

The activation dependence of the effective time scale assures that activation patterns decay slowly between trials (when no input is provided), so that preshape depends little on intertrial intervals. At the same time, the preshape field adjusts quickly to changes in input activation and reacts quickly to input when that input first arrives to a quiescent memory field.

One limitation of our model comes from the fact that the initiation of the movement and its control are not modeled in detail. Thus, the decay of activation in the movement parameter field is not described by the dynamics. In the simulations of the preshaping dynamics, input from activated sites of the movement parameter field is modeled by providing positive input to the memory field for a trial duration, ΔT, which represents an additional parameter. This trial duration affects the absolute level of activation in the memory field (as input is continuously applied), but not the relative amount of activation at different sites of the memory field. During intertrial intervals, the interaction contribution to the preshape dynamics is assumed to be absent.

The preshape dynamics are generalized without difficulty to multiple dimensions, in a manner similar to that used for the Amari (1977) equation. We have simulated two dimensions. The activation field $u_{mem}(x, t)$ is replaced by a two-dimensional version, $u_{mem}(x, y, t)$, and the inhibitory interaction is now controlled by a two-dimensional kernel $w_{mem}(x - x', y - y')$ that can be either a two-dimensional Gaussian profile or a constant function $w_{pre,inhibit}$.

Appendix C

Model Parameter Values

All models have parameters for which values must be determined. (Many experiments have parameters as well, because most effects arise only under a specific set of experimental conditions.) The choice of parameter values for model parameters involves assumptions about the nature of the theory–experiment relationship. The effects we discuss in this article result from the theory regardless of the particular choices for functional form and parameter values. For instance, the principle by which the distance of preshape from the specified pattern of activation determines reaction time applies quite generally for a wide class of parameter values and functional forms. Thus, experimental results that agree with the model are confirmations of the deep structure of the theory and depend little on the procedure for choosing parameter values.

Finding values of the model parameters at which a set of experimental results is well approximated by the model serves two purposes. First, it is an existence proof that shows that there are no hidden properties of the model that prevent good fit of experimental results. Although different experimental settings (different movement parameters, different effectors, different boundary conditions, different movement targets, different sources of sensory information) may naturally require different sets of parameter values, we have tried to use a single set of parameter values for most experimental facts. We preferred approximate fit based on these fixed parameter values to detailed fitting of each individual result, because it shows the effects are generic and highlights how different types of observations can be linked through the model.

Second, within the framework of the theoretical concepts on which the model is based, the determination of model parameter values provides a method of analysis. For instance, determining the size of the localized peaks of activation in the dynamic field for different movement parameters provides information that is interesting per se. As a method of analysis, the determination of parameter values makes use of a number of arguments that establish links between particular experimental signatures and the values of particular parameters: First, the time scale, τ, determines the units of time relative to experimental time units. Second, the global inhibition parameter, h, determines the units of the activation variables and is arbitrary (but must be negative). Third, the strength of preshape effects as a percentage of the reaction time determines the ratio of the strengths of task input, g_{task}, and of specificational input, g_{spec}. Fourth, the width of task input, σ_{mem}, is inferred from metrical distances between choices at which the default distribution measured in the timed movement initiation paradigm changes from monomodal to bimodal (Ghez et al., 1997). Fifth, the noise strength, q, is obtained by comparing the task input width obtained in this way with the observed width of the default distribution in a monomodal case. Sixth, the observation that the width of the individual modes of the default distribution varies little with the distance of the modes (in the case of direction as observed by Favilla, Gordon, Ghilardi, & Ghez, 1990) implies that the three contributions of intrafield interaction, specific input, and task input have comparable width. Seventh, the width of the global inhibitory part of the intrafield kernel equals the kernel length, Δw, and determines the range over which interactions (and thus metrical effects) can be observed. We have assumed that this width matches the entire range of the movement parameters.

The fields were simulated by numerical integration using the Euler procedure and spatial discretization. The integro-differential form of the dynamics is particularly well-behaved, so numerics did not pose much of a problem, except as far as computation time was concerned (as the integrand requires convolution in one or even two dimensions at each time step). The results were obtained on various types of Sun Ultrasparc workstations using Matlab 5.1 running under Unix.

One-Dimensional Field Dynamics

The parameter values used for the simulations of the one-dimensional movement parameter field were as follows: time scale, $\tau = 75$ ms; resting level, $h = -3$; sigmoid, $\beta = 1.5$, $u_0 = 0$; interaction kernel, $w_{excite} = 1.6$, $w_{inhibit} = 1$, $\sigma_w = 10$; task input, $\sigma_{mem} = 10$; specific input, $\sigma_{spec} = 10$. The strengths of these two inputs, g_{task} and g_{spec}, vary with experimental conditions (for instance, as a function of the probability of choice or of stimulus–response compatibility). Specific values used in different simulations are indicated in the figure captions. For the stochastic simulations we adapted the time scale $\tau = 150$ ms (to facilitate the numerics). The noise strength was chosen as $q = 6$. The total range of the parameter values was 200 (arbitrary units), which also determined the total width of the

interaction kernel. Note that because of global inhibition, the balance of excitatory and inhibitory interaction depends on this total range.

The parameter setting for the simulations of the memory field dynamics shown in Figure 10 are as follows: time scale, $\tau_{\text{mem}} = 50$ ms, $A = 0.01$; sigmoid, $\beta = 10$, $u_0 = 0$, input width $\sigma_i = 10$, and strength $g_i = 0.44$; duration of trial, $\Delta T = 10$; kernel, $w_{\text{pre,inhibit}} = 0.011$.

Two-Dimensional Field Dynamics

The two-dimensional field dynamics is assumed to be homogeneous and separable. Thus both the excitatory part of the interaction kernel $w(x - x', y - y')$ and the specific input, $S_{\text{spec}}(x, y)$ are products of Gaussian distributions, depending each on a single dimension only. The width and strength of these factors are model parameters. The width parameters are constrained by experimental information about modality of preshape as in one dimension. To limit the computational time necessary to solve numerically the two-dimensional field equations, parameter spaces were discretized using a larger spatial grid size ($\Delta x = 10$) compared with the one-dimensional case ($\Delta x = 1$). In our formulation this affects the choice of the strength parameters for the interaction kernels (because it fixes the units of the spatial dimensions).

The parameter values for the movement field were as follows: time scale, $\tau = 75$ ms; resting level, $h = -2$; sigmoid, $u_0 = 0$, $\beta = 4$; kernel, $w^x_{\text{excite}} = 2.0$, $w^y_{\text{excite}} = 1.6$ (for both x and y), $w^{xy}_{\text{inhibit}} = 1.5$, $\sigma^x_w = 10$, $\sigma^y_w = 25$; specific input, $g^x_{\text{spec}} = 1.75$, $g^y_{\text{spec}} = 0.7$, $\sigma^x_{\text{spec}} = 10$, $\sigma^y_{\text{spec}} = 25$. The range of parameter values was 200 units in both spatial directions with corresponding kernel size.

The parameters for the memory field, $u_{\text{mem}}(x, y)$, were chosen to generate a monomodal preshape for amplitude, y, and a bimodal preshape for direction, x. In addition, the "normalization" property of Equation B1 ensures that in the case of strongly overlapping inputs (here, for the two amplitude values) the summed preshape strength will not pass a critical activation level, beyond which the field evolves toward a self-stabilized peak. We used a global constant inhibitory interaction kernel, $w_{\text{mem,inhibit}}$, for the simulation shown in Figure 21.

The parameter values for the preshape field were as follows: time scale, $\tau_{\text{mem}} = 50$ ms; sigmoid, $u_0 = 0.5$, $\beta = 25$; strength and width of input $I(x, y)$ from precue (Gaussian distributions centered on cued parameter value), $g^x_i = 1.8$, $g^y_i = 0.72$, $\sigma^x_i = 10$, $\sigma^y_i = 25$; kernel, $w_{\text{mem,inhibit}} = 0.3$.

Appendix D

Hick's Law Derived From the Dynamic Field Model

Consider task environments in which the metric and topology of the different parameter values required under the different conditions do not affect performance. This results when the values are sufficiently separate in the underlying continuous topology so that the interaction between the corresponding field sites is independent of the exact metrical distance. It may also occur if the number of dimensions along which the parameters are distinguished is similar to the number of different parameter values required. In these cases the limit case of the dynamic neural field model is relevant, in which only the total amount of preshape input, not its spatial distribution, matters. Here we show that in this limit case the predictions of the dynamic field model are similar to predictions based on information theoretical accounts such as summarized by the Hick–Hyman law (Hick, 1952; Hyman, 1953). We derive this law by approximating the solutions of a simplified dynamic field model in the limit of homogeneous interaction. Predicted deviations from the pure form of Hick's law are discussed.

Our starting point is the field dynamics Equation A1 with a local excitatory and a global inhibitory interaction (Equation A3). Consider a task environment in which n possible choices of parameter values, $x_i (i = 1, \ldots, n)$, are relevant. Assume that the preshaped field representing these choices consists of n subthreshold peaks at locations, x_i, with width δ. If these peaks interact with each other only through the homogeneous part of the interaction kernel, then the topology of the choices will not matter. This may come about, for instance, because the separations between these peaks are larger than the range of the excitatory interaction, σ_w (see Figure 15). In this limit case we can introduce a coarse-grained description of the dynamic field, in which we integrate the activation in the neighborhood of each parameter value, x_i:

$$v_i = \int_{x_i - \delta/2}^{x_i + \delta/2} u(x)dx. \tag{D1}$$

The task and specific input are treated correspondingly:

$$S = \int_{x_{\text{spec}} - \delta/2}^{x_{\text{spec}} + \delta/2} S(x)dx; \quad P = \int_{x_i - \delta/2}^{x_i + \delta/2} P(x)dx. \tag{D2}$$

This leads to a set of coupled ordinary differential equations,

$$\tau \dot{v}_i = -v_i + ef(v_i) - \sum_{j(\neq i)} wf(v_j) + h\delta + P + S\delta_{i,\text{spec}}, \tag{D3}$$

where the specific information, S, is present only for the activation variable, which represents the specified parameter value (i = spec). (The Kronecker symbol $\delta_{i,\text{spec}}$ is one if the two indices coincide and zero otherwise.) The interaction terms result from integrals over the self-excitation of each peak, summarized by the parameter e, and over the mutual inhibition of different peaks, summarized by the parameter w. Strictly speaking, the functional form of the threshold function as it results from this approximation may differ from the one occurring under the interaction integral (Equation A2). However, the relevant qualitative features (limits of zero at sufficiently negative and one at sufficiently positive activation) remain invariant under this coarse-graining operation.

A further simplification results from the symmetry of this equation: All activation variables, v_i, that do not represent the specified parameter value ($i \neq$ spec) have equivalent dynamics, and we seek only solutions invariant under permutation of these variables. Thus we may replace these $n - 1$ equations by a single representative one for $v = v_i$. Denoting the activation variable that represents the specified parameter value by u, we obtain

$$\tau \dot{u} = -u + ef(u) - nwf(v) + h + P + S, \tag{D4}$$

$$\tau \dot{v} = -v + ef(v) - (n - 1)wf(v) - wf(u) + h + P, \tag{D5}$$

where we have renamed $h\delta$ into h.

We can solve these two equations analytically in the limit case of a step-function threshold,

$$f(u) = \Omega(u) = \begin{cases} 1 & \text{for } u > 0 \\ 0 & \text{else} \end{cases}, \tag{D6}$$

which results from Equation A2 by taking $\beta \to \infty$. The system is then a piecewise linear dynamics.

The reaction time is computed as the time needed for the activation variable u to reach a threshold, u_c. The initial condition is the stable

(*Appendix continues*)

stationary solution obtained when $S = 0$, $P \neq 0$. The transient can be computed by observing the exponential decay toward the stationary stable state at $S \neq 0$, $P = 0$. The piecewise linear dynamics leads to different parameter regimes; the relevant regimes can be identified by arguing about the number and nature of fixed points in the presence of preshape input and in the presence of specific input. We find that the assumptions $h + P > 0$, $h - w < 0$, $h + S + e > 0$ lead to the correct qualitative dynamics. In this case we find

$$RT = \begin{cases} \tau \ln\left(\dfrac{S - P + nw}{h + S + e - u_c}\right) & \text{while } n < \dfrac{h + P + e}{w} \\ \tau \ln\left(\dfrac{h + S + e}{h + S + e - u_c}\right) & \text{for } n > \dfrac{h + P + e}{w} \end{cases}, \quad \text{(D7)}$$

where RT is reaction time. This formula leads to three regimes (see Figure 17 for numerical plots): For intermediate values of $\ln(n)$, the classical Hick formula is approximated, that is, $RT \sim \ln(n)$. Deviations from this form result from the limit of small $\ln(n)$, which leads to an increase stronger than $\ln(n)$: $RT \sim \ln(a + bn)$. The size and range of these deviations depend on the choice of parameters. For sufficiently large values of n, the predicted reaction time saturates at a finite value. The crossover point depends likewise on the model parameters.

Figure 17 also shows how reaction time predicted from this formula becomes smaller for increasing strength of specific input, S, and at the same time the slope of the logarithmic part decreases as well. We have linked the strength of specific input to stimulus–response compatibility, so that this result is in agreement with the reduction in reaction time for increasing stimulus–response compatibility and with the experimental observation that the slope in the Hick–Hyman law decreases with increasing stimulus–response compatibility.

Finally, note that in the derivation only the total amount of inhibitory interaction matters. As long as the limit case of homogeneous interaction (i.e., no topology effects) remains valid, other preshapes than those corresponding to n equally strong choices can be dealt with in the same style. For instance, by mapping the probability of a choice linearly onto preshape strength, P, we obtain the Hyman version of the law in analogous fashion.

Received January 18, 1996
Revision received July 13, 2001
Accepted July 25, 2001 ■